

Progress towards water-soluble triazole-based selective MMP-2 inhibitors†

Cite this: *Org. Biomol. Chem.*, 2013, **11**, 6623

Benjamin Fabre,^a Kamila Filipiak,^{a,b} José María Zapico,^a Natalia Díaz,^c Rodrigo J. Carbajo,^d Anne K. Schott,^d María Paz Martínez-Alcázar,^a Dimas Suárez,^c Antonio Pineda-Lucena,^d Ana Ramos^{*a} and Beatriz de Pascual-Teresa^{*a}

Water solubility is a key aspect that needs to be addressed to obtain drug-like compounds. In an effort to improve the water solubility of our recently reported nanomolar matrix metalloproteinase type 2 (MMP-2) inhibitors based on triazole-substituted hydroxamates, we synthesized a new series of α -sulfone, α -tetrahydropyran and α -piperidine, α -sulfone *clicked* hydroxamates and determined their inhibitory activities against both MMP-2 and MMP-9. The best results were found for **13e**, a water-soluble compound that displays a low nanomolar activity against MMP-2 and is 26-fold less active against MMP-9. This finding allowed us to pursue *in vitro* permeability through the Caco-2 monolayer and opened the possibility of carrying out further preclinical investigations. Docking and MD simulations have been performed in order to rationalize the biological results. The inhibitory activity of this compound against a panel of ten MMPs was determined showing an interesting MMP-2/MMP-1, -8, and -14 selectivity profile. The cytotoxicity and anti-invasive activity of the compounds on highly metastatic human fibrosarcoma tumor cells (HT1080) were determined, showing, at 10 μ M concentration, a decrease in cell invasiveness up to 80%.

Received 20th May 2013,
Accepted 2nd August 2013

DOI: 10.1039/c3ob41046c

www.rsc.org/obc

Introduction

Matrix metalloproteinases (MMPs) are zinc-dependent peptidases involved in the remodeling of the extracellular matrix (ECM).¹ Mammalian MMPs are classified into six subfamilies,² one of them (gelatinases) constituted by MMP-2 and MMP-9. MMP-2 has been associated with several pathologies and especially with cancer.³ While MMP-2 is a validated target in cancer therapy, MMP-9 is considered to be an anti-target in an advanced state of the disease.³ Thus, we are particularly interested in the design of small molecules that selectively inhibit MMP-2 over MMP-9.

We first undertook an exhaustive bibliographic search for hydroxamate-type MMP-2 inhibitors. More than 560 compounds were computationally clustered and classified according to their MMP-2/MMP-9 selectivity.⁴ From this work, we selected the α -sulfone- α -THP core developed by Becker *et al.*,^{5–8} as it displays good PK properties, as well as the most interesting MMP-2/MMP-9 selectivity. We elaborated a *click* chemistry approach to connect this core to fragments chosen to interact with the S1' subpocket, known as the selectivity pocket of MMPs.^{9,10} Following this strategy, we have recently reported a family of *clicked*-hydroxamic acids as potent MMP-2 inhibitors, which display promising selectivity over MMP-9.¹¹ Compounds **1a–d** (Fig. 1) showed the best selectivity profile. Unfortunately, those compounds suffered from low water solubility, which constitutes a drawback for further drug development.

Herein, we report the synthesis and biological evaluation of a related family of *clicked*-hydroxamic acids, designed to improve the drug-like properties of this type of compound, while maintaining their inhibition profile. To this end, two strategies were followed: (a) addition of a polar/charged group at the P1' fragment and/or (b) replacement of the THP ring by a more basic piperidine moiety. The target compounds were synthesized by following the same *click* approach as that used for the synthesis of **1a–d**. Cytotoxicity of the compounds on the HT1080 cell line, as well as their anti-invasive activities,

^aDepartamento de Química y Bioquímica, Facultad de Farmacia, Universidad CEU San Pablo, Urbanización Montepríncipe, 28668 Madrid, Spain.

E-mail: bpaster@ceu.es, aramgon@ceu.es; Fax: (+34) 913510496;

Tel: (+34) 913724724, (+34) 913724796

^bDepartment of Molecular Biology, Faculty of Mathematics and Natural Sciences, The John Paul II Catholic University of Lublin, 20-718 Lublin, Poland

^cDepartamento de Química Física y Analítica, Universidad de Oviedo, C/Julián Clavería, 8. 33006 Oviedo, Asturias, Spain

^dStructural Biology Laboratory, Medicinal Chemistry Department, Centro de Investigación Príncipe Felipe, C/Eduardo Primo Yúfera 3, 46012 Valencia, Spain

†Electronic supplementary information (ESI) available: Time evolution of the Root-Mean-Square Deviation (RMSD) for the protein backbone atoms of the MD trajectory (Fig. S1) and ¹H and ¹³C NMR spectra of compounds **1e–i** and **13a–j**. See DOI: 10.1039/c3ob41046c

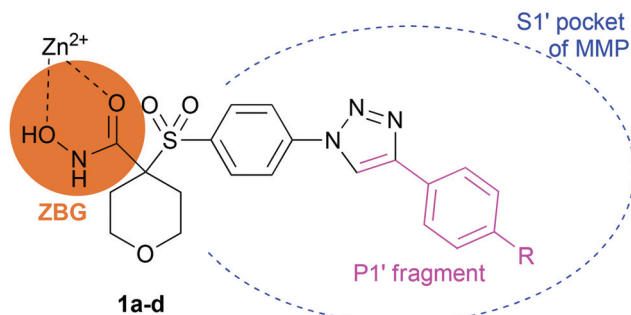


Fig. 1 Chemical structures of compounds **1a–d**.¹¹ To obtain compounds **1a–d**, different ethynyl containing fragments (called P1' according to the Schechter and Berger notation¹²) were *clicked* to the azide containing the Zinc Binding Group (ZBG). This approach allowed rapid screening of the MMPs S1' pocket by the diverse P1' fragments.

was determined. The interesting water-soluble compound **13e** was chosen for screening its inhibitory activity against eight MMPs and a mixture of HDAC, as well as for transport experiments across the Caco-2 monolayer.

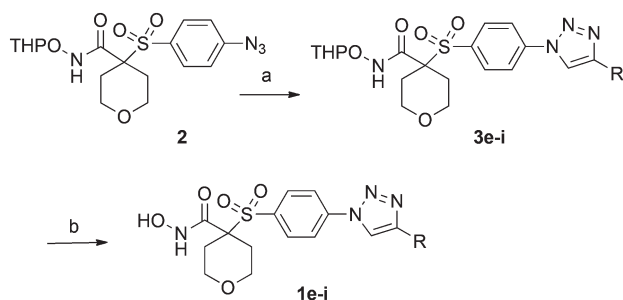
Results and discussion

Chemistry

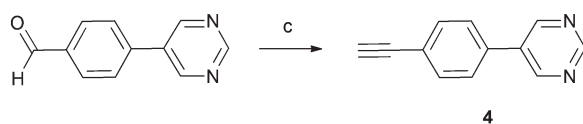
In a first attempt to improve the water-solubility of **1a**, the biphenyl moiety was replaced by basic groups (aniline, pyridine, pyrimidine, piperidine and morpholine derivatives), which were isolated as hydrochloride salts in **1e–i**. The synthetic route for **1e–i** is depicted in Scheme 1.

Azide **2**¹¹ was converted into triazole derivatives **3e–i** using copper sulphate pentahydrate and sodium ascorbate as the standard catalyst system for the copper(I)-catalyzed azide-alkyne cycloaddition (CuAAC). Acidic removal of the THP group led to hydrochloride salts **1e–i**. The alkynes necessary

Scheme 1a Synthesis of **1e–i**



Scheme 1b Synthesis of alkyne **4**



Scheme 1 Synthesis of **1e–i** and **4**. Reagents and conditions: (a) $\text{CuSO}_4 \cdot 5\text{H}_2\text{O}$ (0.06 eq.), sodium ascorbate (0.20 eq.), alkyne, 1 : 1 $t\text{BuOH-H}_2\text{O}$; (b) 4 M HCl -dioxan; (c) BOR, K_2CO_3 , $\text{MeOH-CH}_2\text{Cl}_2$.

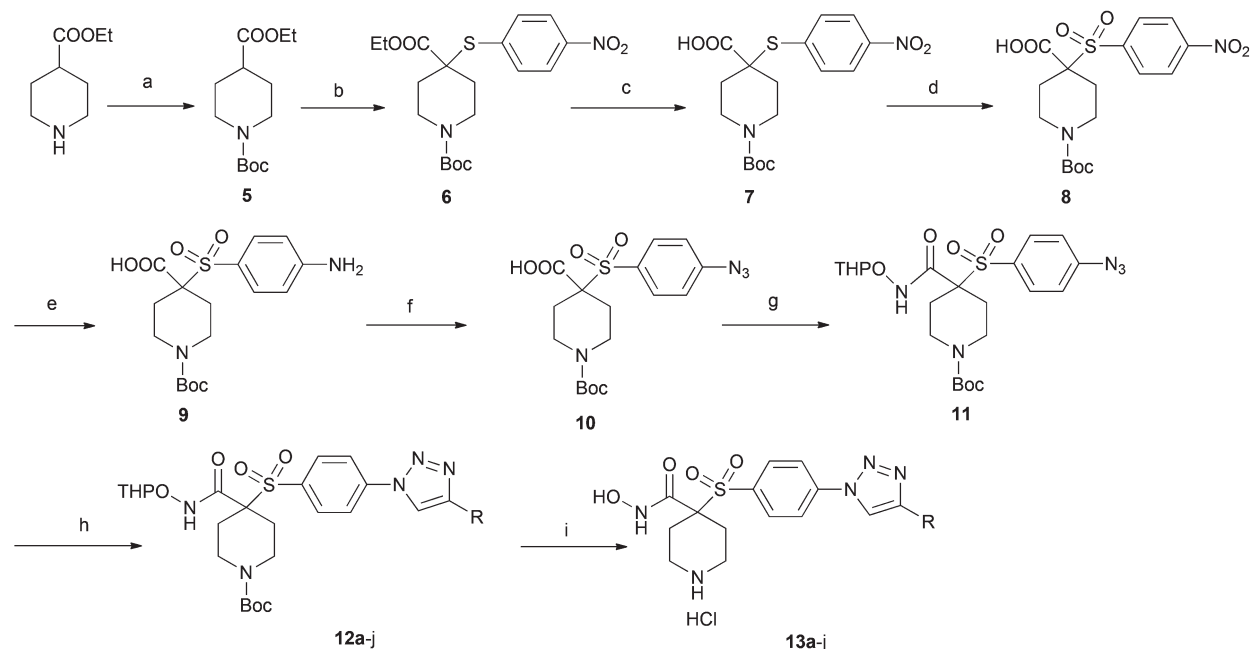
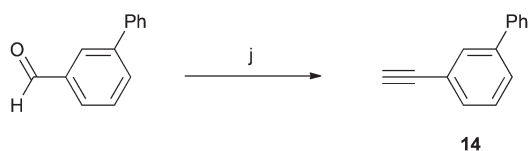
for the synthesis of **3f–h** were obtained as described in the literature (refer to the Experimental section). 5-(4-Ethynylphenyl)-pyrimidine **4**, necessary for the synthesis of **3i**, was synthesized as shown in Scheme 1b, starting from 4-(pyrimidin-5-yl)-benzaldehyde, making use of the Bestmann–Ohira reagent (BOR).¹³

A second series of MMP-2 inhibitors **13a–j**, based on a hydroxamate ZBG and a piperidine basic moiety, were synthesized. The P1' fragments selected in compounds **13a–d** were those that gave the best results in our previous work in this field.^{11,14} In order to increase the basicity of the molecule, we synthesized **13e**, where a dimethylamino substituent was introduced at this position. To screen the gelatinase S1' pockets we also selected a series of alkynes varying in polarity, rigidity, orientation and length.

α -Piperidine- α -sulfone hydroxamic acids **13a–j** were synthesized as depicted in Scheme 2. Ethyl isonipecotatate was protected with the corresponding Boc-amine **5**.¹⁵ Subsequent deprotonation with LDA and sulfonylation with bis(*p*-nitrophenyl) disulfide afforded sulfide **6**. MCPBA oxidation of the sulfide to the corresponding sulfone, followed by saponification of the ester, brought about the elimination of the *p*-nitrophenylsulfone group. Consequently, we carried out first the saponification of **6** to obtain the carboxylic acid **7**, which was then oxidized with MCPBA to give sulfone **8**. This compound appeared to suffer partial decarboxylation during chromatography on silica gel or recrystallization. Subsequent hydrogenation yielded aniline derivative **9**, which was converted into azide **10** by reaction with *tert*-butyl nitrite followed by *in situ* reaction of the formed diazonium salt with azidotrimethylsilane as the azide source. Amide coupling between carboxylic acid **10** and *O*-(tetrahydro-2*H*-pyran-2-yl)hydroxylamine using EDCI/HOBt as the coupling system gave the THP-protected hydroxamic acid **11**. CuAAC, using the standard catalyst system, led to the triazole family **12a–j**. Subsequent acidic removal of both BOC and THP groups afforded the corresponding hydrochloride salts **13a–j**. An alternative and shorter sequence, where **11** was first deprotected and then coupled to the selected alkynes, was also investigated. The first route was preferred, as it proved to be more efficient in terms of yields and handling (especially for purifications). For the synthesis of **13j**, the alkyne derivative **14** was prepared from [1,1'-biphenyl]-3-carbaldehyde using BOR (Scheme 2b).

NMR studies

Intermolecular interaction experiments waterLOGSY¹⁶ and STD¹⁷ were used recently in the characterization of novel inhibitors binding to MMP-2.¹¹ Here we have applied a similar methodology for the characterization of the protein–ligand interaction between MMP-2 and compounds **13a**, **13b** and **13e**. Although both STD and waterLOGSY are ligand-based techniques that provide equivalent binding information, the latter technique proved to be more adequate in the current study. The low solubility in water of compounds **13a–b** resulted in concentrations much below the ideal protein : ligand ratio for STD experiments (1 : 100) resulting in NMR spectra presenting

Scheme 2a. Synthesis of **13a-j**Scheme 2b. Synthesis of **14**

Scheme 2 Synthesis of **13a-j** and **14**. *Reagents and conditions:* (a) Boc_2O , I_2 (0.10 eq.), CH_3CN , 100%; (b) (i) LDA, 0°C , THF; (ii) *p*-nitrophenyl disulfide, 73%; (c) NaOH, H_2O –EtOH, 93%; (d) MCPBA, CH_2Cl_2 , 78%; (e) black Pd (2% mol.), H_2 (60 psi), EtOH, 99%; (f) *t*BuONO, TMSN₃, CH_3CN , 69%; (g) THPONH₂, EDCI, HOBT, NMM, DMF, 48%; (h) $\text{CuSO}_4 \cdot 5\text{H}_2\text{O}$ (0.06 eq.), sodium ascorbate (0.20 eq.), alkyne, 1 : 1 *t*BuOH– H_2O ; (i) 4 M HCl–dioxan; (j) BOR, K_2CO_3 , MeOH– CH_2Cl_2 , 71%.

very low sensitivity, while the 1 : 20 ratio indicated for waterLOGSY was attainable and yielded reasonably good spectra. Under our experimental conditions, compounds **13a**, **13b** and **13e** did not show clear evidence of positive interaction with MMP-2 in the waterLOGSY experiments. The negative result observed for compound **13a** could be attributed to its very low solubility in water, evidenced by the absence of recognizable signals in the simple 1D ^1H NMR spectrum. The absence of a positive intermolecular interaction for compound **13e** could be expected for a molecule presenting high affinity for the protein and therefore out of the normal weak-binder detection range of the waterLOGSY experiment. These false negatives can still be detected *via* competition experiments with the use of a binding reporter, a molecule known to interact with the biomolecule at the site of interest. In our case we evaluated the binding of **13e** in the presence of 2*R*-[4-(biphenylsulfonyl)-amino]-*N*-hydroxy-3-phenylpropinamide (BiPS), a commercially available MMP-2/-9 inhibitor ($\text{IC}_{50/\text{MMP-2}}$: 17 nM; $\text{IC}_{50/\text{MMP-9}}$: 30 nM). The waterLOGSY experiment of MMP-2–BiPS yielded the expected positive signals for the inhibitor, seeing its resonances reduced over 60% upon addition of compound **13e** to

the MMP-2–BiPS mixture. These results indicate that **13e** binds to MMP-2 at the catalytic site, and with an affinity towards MMP-2 in a similar range to that of BiPS.

Biological activity

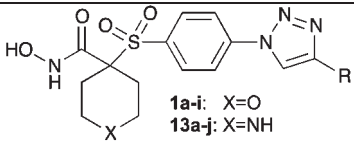
Water solubility and inhibitory activity. The aim of synthesizing this new series of triazole-substituted hydroxamates was to improve the water solubility of the THP-based compounds previously reported (**1a–d**). Therefore, an evaluation of the hydrophilic properties of the target compounds was first undertaken. Table 1 displays the estimated $c \log D$ values at pH 7.4 of the synthesized hydroxamic acids. Compared to **1a–d**, the new piperidine based compounds **13a–j** show considerably increased calculated hydrophilicity, with a drop of about two log units in the $c \log D$ in most cases. Next we determined the kinetic solubility in water of THP derivatives **1a–e** and **13a–e** by UV spectroscopy, following the method described by Mobashery.¹⁸ The addition of a polar group at the P1' fragment in compounds **1e–i** did not improve the water solubility of these THP-based inhibitors, which showed a similar behavior as **1a–d**. In accordance with the $c \log D$ estimations, the water

Table 1 MMP inhibition potencies, ligand efficiency (LE), $c \log D_{7.4}$, solubility in water, and % of inhibition of invasion for compounds **1a–i** and **13a–j**

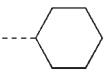
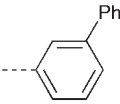
1a–i: X=O
13a–j: X=NH

Cpd	R	MMP-2 ^a (nM)	MMP-9 ^a (nM)	Selectivity $\frac{IC_{50}^{MMP9}}{IC_{50}^{MMP2}}$	MMP-2 LE ^c	$c \log D_{7.4}$ ^d	Solubility in water ^e ($\mu\text{g mL}^{-1}$)	Cytotoxicity ^j (μM)	Inhibition of cell invasion ^k (%)
1a		1.4 ^b	98.0 ^b	70.0 ^b	0.34	3.96	<10 ^f	10	63
1b		2.1	24.9	11.9	0.34	4.75	<10 ^f	1	64
1c		0.3 ^b	11.3 ^b	37.7 ^b	0.41	2.22	<10 ^f	10	50
1d		1.6	20.2	12.6	0.33	3.87	nd ^g	1	32
1e		0.4	4.3	10.8	0.39	2.36	<10 ^f	10	28
1f		0.2	1.8	9.0	0.37	2.79	nd ^g	5	36
1g		0.5	0.8	1.6	0.35	2.14	nd ^g	10	41
1h		2.0	62.4	31.2	0.33	3.28	nd ^g	1	47
1i		2.7	31.0	11.5	0.32	2.21	nd ^g	5	51
13a		13.6	95.3	7.0	0.30	2.13	— ^h	10	64
13b		21.0	41.7	2.0	0.30	2.91	~135 ⁱ	1	19
13c		3.6	28.4	7.9	0.36	0.39	nd	10	48
13d		5.7	41.2	7.2	0.31	2.04	— ^h	1	— ^l
13e		1.7	43.9	25.8	0.36	0.53	996 ± 98	10	37
13f		1.9	17.7	9.3	0.39	0.64	nd	10	80
13g		4.4	14.5	3.3	0.37	0.64	nd	50	48
13h		6.8	44.0	6.5	0.36	0.64	nd	10	29

Table 1 (Contd.)



1a-i: X=O
13a-j: X=NH

Cpd	R	MMP-2 ^a (nM)	MMP-9 ^a (nM)	Selectivity $\frac{IC_{50}^{MMP9}}{IC_{50}^{MMP2}}$	MMP-2 LE ^c	$c \log D_{7.4}$ ^d	Solubility in water ^e ($\mu\text{g mL}^{-1}$)	Cytotoxicity ^f (μM)	Inhibition of cell invasion ^k (%)
13i		10.5	188.6	18.0	0.37	0.84	nd	5	nd
13j		>700	Nd	nd	nd	2.13	nd	5	nd

^a Determined using the colorimetric assay. Enzymatic data are mean values from three independent experiments. SD are within $\pm 10\%$. ^b Values from the literature.¹¹ ^c Ligand efficacy (LE) was calculated using the expression (IC_{50} were taken for K_i values): $LE = \frac{\Delta G_{\text{binding}}}{N_{\text{heavy atoms}}} = \frac{-RT \ln K_i}{N_{\text{heavy atoms}}}$. ^d Calculator Plugins were used for $c \log D$ calculations, Marvin 5.9.1, 2012, ChemAxon (<http://www.chemaxon.com>). ^e Determined by UV spectroscopy (see the Experimental section). ^f Very low solubility. The absorbance of the saturated solution is at the same level of the blank. ^g Not determined. Qualitatively similar to other THP-based analogues. ^h Not enough water soluble to be strictly determined. ⁱ Non-linear behavior. ^j Highest non-cytotoxic concentration on the HT1080 cell line. ^k Inhibition of HT1080 cell invasion at the highest non-cytotoxic concentration of the inhibitor, in comparison to the solvent control (0.1% DMSO). In the case of compound **13g** the tested concentration was 10 μM . SD were within $\pm 15\%$. ^l No inhibition in the invasion assay.

solubility of the piperidine derivatives appeared to be qualitatively better than the THP analogues. In particular, compound **13e**, bearing a dimethylaniline at position P1', was isolated as a dichloride salt and was soluble in water at concentrations reaching the mg mL^{-1} range.

Ligand efficiency is a useful parameter to select a lead compound for further optimizations.¹⁹ Compounds with high LE tend to be small molecules that allow more efficient growth during the lead optimization process. Both series showed good LE (>0.30), which is mainly due to the strong zinc ion-hydroxamate interaction.²⁰

In our previous studies, we observed that compounds **1a-d** inhibited MMP-2 at low nM concentrations.¹¹ We expected that the substitution of the THP ring by a piperidine would have a minor effect on their potency against the two gelatinases, as these groups are expected to be solvent exposed according to the predicted binding modes¹¹ and X-ray structures of related inhibitors.^{6,21,22} In fact, **13a-d** kept IC_{50} values in the nM range against the two gelatinases (Table 1). Nevertheless, we noticed that the substitution of the THP ring by a piperidine led to a slight loss of potency against MMP-2, while maintaining the same inhibitory activity against MMP-9. For instance, compound **13a** was ten times less active in MMP-2 than the homologous THP derivative **1a**. Similar results were observed for compounds **13b-d**. Such a loss of potency was observed in similar β -sulfone, α -tetrahydropyran hydroxamate derivatives.⁵ In contrast, when R is an *N,N*-dimethylamino moiety (**1e** and **13e**) both compounds exhibited similar IC_{50} values against MMP-2, whereas the THP-based derivative was 10-fold more potent on MMP-9. Thus, **13e** presents a very

encouraging therapeutic profile, with an activity against MMP-2 in the low nanomolar range, ~ 26 -fold selectivity against MMP-9, and a good solubility in water.

Comparing the IC_{50} values presented in Table 1, some conclusions can be drawn about the SAR of these compounds. The *para* position of the phenyl ring linked to the triazole moiety admits a variety of groups, leading to potent inhibitors of MMP-2, with IC_{50} values below 21 nM. In contrast, **13j**, with *m*-phenyl substitution, did not show any inhibition of MMP-2 at 700 nM. This is in accordance with the tunnel-like shape of the gelatinase S1' pocket.²³ The fluorine atom is an interesting probe in medicinal chemistry due to its ability to give interactions with proteins^{24,25} and fluorine scans have been used to map the fluorophilicity of some enzymes.^{26,27} Thus, we substituted all the positions of the mentioned phenyl ring by a fluorine atom (**13f-h**). Interestingly, the *para* substituted compound (**13f**) was three times more active than the *ortho* substituted compound (**13h**) and displayed the best MMP-2/MMP-9 selectivity (almost three times more selective than the *meta* substituted analogue **13g**). Looking at the IC_{50} values of **1b**, **1h**, **1i**, **13b** and **13i**, we observed that the insertion of a bulkier group at S1' pocket decreases the inhibitory activity against both gelatinases. For instance, passing from a flat pyridine group (**13f**) to a piperidine ring (**13h**) led to a loss of one order of magnitude in the IC_{50} value against MMP-2. Substitution of the distal phenyl ring in **1a** by a pyridine ring decreased 7-fold the IC_{50} value against MMP-2, and by more than 50-fold the IC_{50} value against MMP-9. A similar change occurred when a pyrimidine group replaces the distal phenyl ring (**1g**). This increase of potency could be explained by the different

electronic distribution of the conjugated rings, which can affect their solvation in complex with the enzyme. It has to be considered that the back doors of the S1' pockets in gelatinases, where the distal ring is expected to be located upon binding, are solvent accessible. On the other hand, MMP-9 displays an Arg at position 143 (1HOV numbering) of its S1' back door, whereas MMP-2 presents a smaller Thr. This difference can also account for the higher MMP-2/MMP-9 selectivity displayed by **1g**.

In vitro invasion assay. It is well established that MMPs promote cell invasion through degradation of the extracellular matrix.^{28–30} Therefore we subjected our inhibitors to an *in vitro* invasion assay against highly metastatic human fibrosarcoma tumor cells (HT1080). Cytotoxicity against this cell line was first determined in order to select the appropriate concentration to be used in the invasion experiment. These data are presented in Table 1.

Inhibition of HT1080 cell invasion at the highest non-cytotoxic concentration of all inhibitors was measured using a fluorimetric QCM ECMatix Cell Invasion Assay (Millipore). The majority of the compounds showed good anti-invasive activity, superior to 30% at concentrations lower than or equal to 10 μ M, which, in comparison with a commercially approved MMP inhibitor, doxycycline hyclate³¹ (50% inhibition at 80 μ M), constitutes a very promising result. Compounds **1b** (64% inhibition at 1 μ M), **1h** (47% inhibition at 1 μ M) and **13f** (80% inhibition at 10 μ M) displayed particularly good anti-invasive activities. Although **13e** displayed lower anti-invasive activity (37% inhibition at 10 μ M), it can still be considered a good result, which highlights its interest for further development.

For further biological experiments (inhibition of a panel of metalloproteases and permeability experiments) we chose among the potent MMP-2 inhibitors those that displayed a good MMP-2/MMP-9 selectivity (>20), which is of primary importance as explained in the Introduction. Four compounds are outstanding in that sense: **1a** and **1c**, studied in a previous work,¹¹ as well as **1h** and **13e**. As **13e** shows good solubility in water and offers more opportunities for further growing the molecule than **1h** (reflected by a higher LE), this compound was preferred.

Table 2 summarizes the selectivity profile of **13e** against a panel of eight MMPs. We include for comparison the same data previously reported for **1a** and **1c**.¹¹

Hydroxamate **13e** almost discriminates MMP-8, -14 from MMP-2, two metalloproteinases considered as anti-targets in

cancer therapy.³ **13e** was found to have no measurable potency against MMP-1 ($IC_{50} > 10\,000$ nM) and a much lower activity (825.4 nM) against MMP-7. This is an expected result since these two MMPs have both small S1' pockets.⁹ It is also a desirable result, because the painful joint-stiffening musculoskeletal side effect observed in patients treated with broad spectrum MMPis has been associated with the inhibition of MMP-1. Moreover, **13e** displays high potency against MMP-13, an enzyme whose upregulation is implicated in several diseases, such as cancer, osteoarthritis, and cardiovascular diseases.⁷ The inhibition of this enzyme has been described as an effective strategy in the treatment of these diseases. In fact, dual MMP-1, -14 sparing, MMP-13 selective α -sulfone hydroxamates have been recently reported by Becker *et al.* as a safe means of treating osteoarthritis, which they refer to as the dual-sparing hypothesis.⁸

On the other hand, we also determined the inhibitory activity of **13e** against a HeLa nuclear extract of histone deacetylases (HDACs), other zinc-dependent proteases. It is interesting to mention that **13e** is inactive against HDACs, whose catalytic center is formed by a narrower tunnel-like pocket,^{32,33} and therefore, this was an expected and desired result.

From all these data, **13e** appears to be the most interesting compound we have found up to now. It slightly improves the good selectivity profile displayed by the highly lipophilic compound **1a** while ameliorating the LE for MMP-2, and strongly improving the solubility in water. In addition, from a drug design point of view, **13e** contains a dimethylamino group, which offers better opportunities than the phenyl ring present in **1a**, to explore the S1' pocket with the final aim of further improving the selectivity profile.

Caco-2 permeability. Compound **13e**, being the most soluble inhibitor, was chosen for transport experiments to evaluate its intestinal permeation. For this, permeation experiments through human colorectal carcinoma-derived cells (Caco-2)³⁴ were performed at 37 °C for 2 h. It is interesting to note that Caco-2 permeability assays with our prior reference compound (**1a**) failed due to its low solubility in water. The results demonstrate that the transport across Caco-2 was present in both directions (apical to basolateral, basolateral to apical), with apparent permeability coefficients (P_{app}) of $0.5 \pm 0.017 \times 10^{-6}$ cm s⁻¹ (A to B) and $0.48 \pm 0.17 \times 10^{-6}$ cm s⁻¹ (B to A). These relatively low values make **13e** similar to approved drugs such as chlorothiazide (0.15×10^{-6} cm s⁻¹ (A to B), 50–60% absorption in oral administration) or atenolol ($\sim 0.4 \times 10^{-6}$ cm s⁻¹, 50% absorption in oral administration).^{35,36} The efflux ratio ($P_{app,ba}/P_{app,ab}$) of 0.96 suggests the presence of passive type transport with no involvement of an efflux pump which is typical of the majority of orally administered drugs. This is an encouraging result for undertaking future *in vivo* biological evaluations.

Computational setting

Docking. To rationalize the SAR discussed above, we performed docking studies with compounds **1a–i** and **13a–j**. We chose structure 10 of 1HOV PDB³⁷ to model MMP-2, as in this

Table 2 Inhibitory activity (IC_{50} values,^a nM) for compounds **1a**, **c**^b and **13e** towards a panel of MMPs ("–1" corresponds to MMP-1, "–3" to MMP-3, etc.)

Cpd.	-1	-3	-7	-8	-10	-12	-13	-14
1a	>10 ³	17.2	>10 ²	>10 ²	51	3.2	0.9	65
1c	>10 ³	9.6	70	6.1	7.8	1.2	1.4	8.2
13e	>10 ³	50.5	825.4	202.0	44.5	4.8	3.2	285.8

^a Enzymatic data are mean values from two independent experiments. SD is within $\pm 10\%$. ^b Values from the literature.¹¹

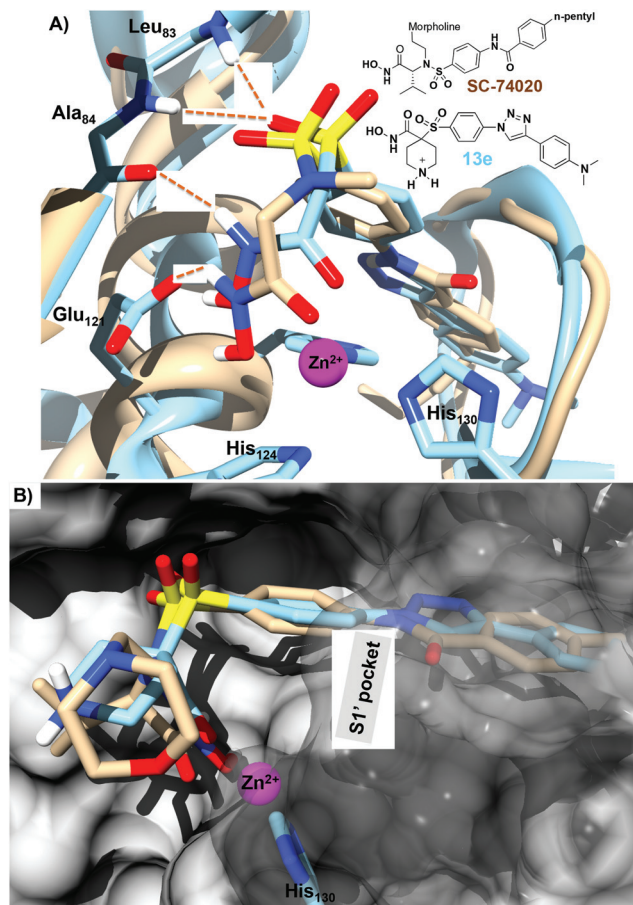


Fig. 2 Superimposition of the lowest energy binding pose for **13e** (light blue) inside MMP-2 and 1HOV (**SC-74020** sandy brown). (A) The H-bond interactions (orange dashed lines) and the bicoordination of the catalytic zinc ion (magenta), predicted for **13e** in docking studies. The ethylmorpholine group (**SC-74020**) and the piperidine ring (**13e**) have been removed. (B) P1' fragments from **13e** and **SC-74020** enter deep into the S1' pocket. The piperidine moiety from **13e** points toward the solvent.

structure, **SC-74020**, a potent MMP inhibitor, interacts with the S1' pocket, ensuring its right opening. For the same reason, 2OW1 PDB²¹ was taken for the MMP-9 structure. The same methodology was followed for all compounds as that described in the Experimental section.

All compounds except **1f-g**, **13a** and **13j** gave good docking in both MMP-2 and MMP-9, and presented the expected binding characteristics (refer to Fig. 2): (1) bicoordination of the catalytic zinc ion by the two-hydroxamic acid oxygens. The cutoff for Zn²⁺ coordination was set to 2.64 Å, as this is the highest distance observed in X-ray structures of MMPs inhibited by a hydroxamic acid, with a resolution lower than or equal to 2 Å; (2) a H-bond between the catalytic Glu₁₂₁ (1HOV numbering is used here) and the hydroxamate OH group; (3) a H-bond between the Ala₈₄ backbone and the hydroxamate NH group; (4) one or two H-bonds between the sulfone group and Leu₈₃ and/or Ala₈₄ backbones; (5) hydrophobic interactions between the P1' fragments and the gelatinase S1' pockets (Leu₈₃, Leu₁₁₆, Val₁₁₇, His₁₂₀, Ala₁₃₆, Leu₁₃₇, Tyr₁₄₂, Thr₁₄₅,

common to MMP-2 and MMP-9, Thr₁₄₃, Phe₁₄₈ specific to MMP-2 and Arg₁₄₃ only present in MMP-9).

A few additional observations are worth mentioning here. First, **13j** failed to correctly dock inside MMP-2, in accordance with the biological results reported above (Table 1). When the *m*-biphenyl moiety fits into the S1' pocket, the hydroxamate group is not well oriented to chelate the catalytic zinc ion and establishes the H-bonds listed above (2 and 3). Secondly, **1f-g** and **13a** were not predicted to have good binding to MMP-9. The flat and rigid 4-phenylpyridyl, 4-phenylpyrimidinyl or 4-biphenyl groups do not enter deep into the S1' pocket and the H-bond established by the sulfone group is lost. In solution, an induced-fit effect is expected, in agreement with the good inhibitory activity shown by **13a** against MMP-9, and docking results inherent in the particular MMP-9 conformation used for this simulation. In accordance with the X-ray structures of related inhibitors in different MMPs,^{6,21,22} the piperidine moiety points toward the bulk solvent, and appears to be a good site for improving the PK properties of these compounds. The fourth point comes from the superimposition of the best poses of compounds **13e** in MMP-2 and **SC-74020** described in 1HOV. As expected, the triazole moiety mimics the amide group present in **SC-74020**. Interestingly, various rotamers for **SC-74020**, coming from the amide flip, are observed in solution.³⁷ However, the triazole moiety rigidifies this bond and, in all the docking poses, only one possible rotamer is observed (Fig. 2). In this way, the 1,4-diphenyl-1,2,3-triazole adopts the curved shape that best matches with the twisted tunnel that forms the S1' pocket. Thus, the entropic contribution to the binding energy should be improved. Finally, in agreement with the biological results (Table 1), our docking suggests that free space is left in MMP-2 and in MMP-9 for bulkier substitution in the *para* position of the 4-phenyl-1,2,3-triazole group.

Molecular dynamics of 13e in MMP-2. A 100 ns Molecular Dynamics (MD) simulation of the MMP-2:**13e** complex in water was carried out by following the protocol described in the Experimental section.

Inspection of the time evolution of the RMSD values (Fig. S1†) confirms that the trajectory is structurally equilibrated after ~20 ns. The overall fold characteristic of the catalytic domain of the MMPs⁹ is well maintained during the simulation, as confirmed by the average RMSD value computed for the backbone atoms during the last 80 ns (2.3 ± 0.3 Å).

In order to explore whether the interactions encountered in docking experiments remain throughout MD simulations, we analyzed the H-bonds and VdW contacts established between MMP-2 and **13e**. Fig. 3 summarizes these observations.

During the MD simulation, **13e** maintains the extended conformation observed in the lowest energy poses from previous docking studies. On the one hand, the distorted bipyramidal coordination mode around Zn₁, in which the ion is chelated to the hydroxamate from **13e**, is perfectly stable all along the MD simulations, confirming that our mixed parameterization of the Zn₁...**13e** interaction reproduces well the most likely coordination mode.³⁸ In addition, the negatively charged

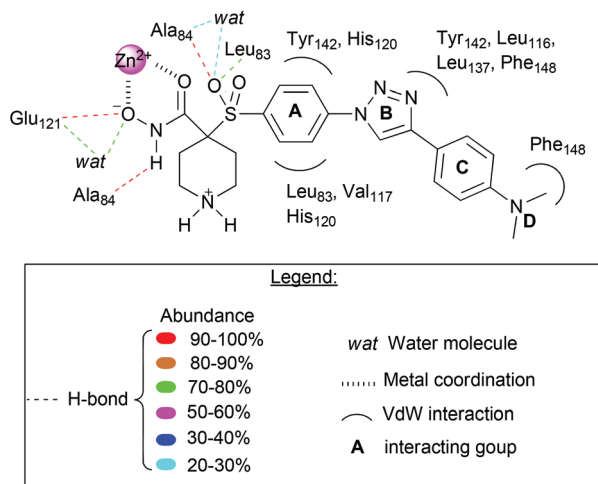


Fig. 3 Interactions (H-bond and VdW) observed between **13e** and MMP-2, during the MD simulation. Abundances of interactions found during the simulation are given according to a color scale.

oxygen from the hydroxamate group interacts with the carboxylic acid from Glu₁₂₁ (1HOV numbering) through a direct H-bond (100% abundance) and a water-bridged H-bond (70% abundance). Similarly, the N-H of the hydroxamate group keeps its direct H-bond contact with the carbonyl of Ala₈₄ (>92%).

Other polar contacts involve one oxygen of the **13e** sulfone group, which acts as an H-bond acceptor in an interaction with the N-H of Ala₈₄ (98% abundance) and the N-H group of Leu₈₃ (79% abundance). On the other hand, the piperidine moiety of **13e** remains solvent-accessible during the MD simulations, while the flat lipophilic chain forms a very stable hydrophobic cluster with the side chains of an array of non-polar residues (Leu₈₃, His₁₂₀, Leu₁₁₆, Val₁₁₇, Leu₁₃₇ and Tyr₁₄₂ common to the two gelatinases and Phe₁₄₈ specific to MMP-2) that constitute the S1' pocket (these VdW contacts present >95% abundance).

Conclusions

We have synthesized a new series of α -piperidine- α -sulfone hydroxamic acids with the aim of improving the water solubility of our previously reported potent α -sulfone- α -tetrahydropyran hydroxamate MMP-2 inhibitors.¹¹ The click approach developed by our group allowed the discovery of **13e**, a promising lead compound with potent inhibition of MMP-2 (IC_{50} = 1.7 nM), a good selectivity profile over MMPs and a promising MMP-2/MMP-9 selectivity (~26), improved LE index and drug-like properties (solubility in the mg mL⁻¹ range) compared to our previously described hydroxamates. **13e** was predicted, according to MD simulations, to bind to MMP-2 maintaining the H-bonds and VdW interactions experimentally observed for **SC-74020**, a similar hydroxamate inhibitor. Based on these encouraging results, further experiments and computational

investigations are under development with the aim of improving the MMP-2/MMP-9 selectivity profile of this compound.

Experimental section

Chemistry

General procedures. Dry solvents were distilled before use and dried by standard methods: THF from Na/benzophenone; CH₂Cl₂ and MeCN, from CaH₂. Dry MeOH was bought from Sigma-Aldrich. All commercially available reagents were used without further purification. Melting points (uncorrected) were determined using a Stuart Scientific SMP3 apparatus. Infrared (IR) spectra were recorded with a Perkin-Elmer Spectrum 100 FT-IR spectrophotometer, using KBr as a solid matrix. ¹H and ¹³C NMR data were recorded either using a Bruker DPX 300 MHz BACS60 or a Bruker Avance III 400 MHz instrument. Chemical shifts (δ) are expressed in parts per million relative to solvent resonance as the internal standard; coupling constants (J) are in hertz. Mass spectra were run using a Bruker Esquire 3000 mass spectrometer (ESI-IT). Analytical purity of the tested compound was determined either by High-Performance Liquid Chromatography coupled to Mass Spectroscopy (HPLC-MS) or by elemental analyses. HPLC-MS experiments were carried out using Synthelia Organics SL 1100 HPLC (Xterra MS C18 5 μ m reverse phase columns) coupled to a 1946D MS detector, both from Agilent. Elemental analyses (C, H, N, S) were performed using a LECO CHNS-932 apparatus at the Microanalyses Service of the Universidad Complutense de Madrid. Thin-layer chromatography (TLC) was run on Merck silica gel 60 F-254 plates, and Merck silica gel 60 (230–400 mesh) was used for flash chromatography.

General procedure for the preparation of triazoles 3a-i

A mixture of **2** (160 mg, 0.39 mmol), the corresponding commercially available alkyne (1.10 eq.), freshly made aqueous 0.1 M CuSO₄·5H₂O solution (234 μ L, 0.06 eq.) and 0.5 M sodium ascorbate solution (156 μ L, 0.20 eq.) in 1:1 *t*BuOH-water (3–5 mL) was stirred at rt under argon for 16–24 h. The reaction mixture was partitioned between CH₂Cl₂ and water. The organic layer was washed with 15% aqueous ammonia, water and brine, dried over anhydrous MgSO₄, filtered and evaporated. The crude product was purified by column chromatography.

For the synthesis of **1a-d**, refer to the literature.¹¹

4-((4-(4-(Dimethylamino)phenyl)-1H-1,2,3-triazol-1-yl)-phenyl)sulfonyl)-N-((tetrahydro-2H-pyran-2-yl)oxy)tetrahydro-2H-pyran-4-carboxamide (3e). Following the general procedure for the preparation of triazoles **3a-i**, from commercially available 4-ethynyl-*N,N*-dimethylaniline, and using CH₂Cl₂-MeOH (0.6% MeOH) as an eluent for chromatography, triazole **3e** (96 mg, 44%) was obtained as a pale orange solid, mp 142–143 °C (dec.). IR (KBr): 3229, 2952, 1692 cm⁻¹; ¹H NMR (300 MHz, CDCl₃) δ 1.64–1.72 (m, 3H), 1.70–1.90 (m, 3H), 2.14 (d, J = 13.1 Hz, 2H), 2.31 (td, J = 12.7, 4.7 Hz, 2H), 3.00 (s, 6H), 3.50 (td, J = 12.0, 3.0 Hz, 2H), 3.69–3.73 (m, 1H), 3.97–4.03

(m, 3H), 5.04 (s, 1H), 6.78 (d, $J = 8.9$ Hz, 2H), 7.76 (d, $J = 8.9$ Hz, 2H), 8.01 (s, 4H), 8.14 (s, 1H), 9.62 (s, 1H); ^{13}C NMR (75.4 MHz, CDCl_3) δ 18.2, 24.9, 27.8, 28.3, 28.5, 40.4, 62.4, 64.2, 64.4, 70.2, 102.0, 112.4, 115.4, 117.4, 120.1, 127.0, 132.1, 133.2, 141.5, 149.7, 150.8, 163.5; MS, m/z : 556.2 $[\text{M} + \text{H}]^+$.

4-((4-(4-(Pyridin-4-yl)phenyl)-1H-1,2,3-triazol-1-yl)phenyl)sulfonyl)-N-((tetrahydro-2H-pyran-2-yl)oxy)tetrahydro-2H-pyran-4-carboxamide (3f). Following the general procedure for the preparation of triazoles **3a-i**, from 4-(4-ethynylphenyl)pyridine,³⁹ and using CH_2Cl_2 -MeOH (2% MeOH) as an eluent for chromatography, triazole **3f** (168 mg, 73%) was obtained as a white solid, mp 219–220 °C (dec.). IR (KBr): 3144, 2952, 1697, 1599 cm^{-1} ; ^1H NMR (300 MHz, $\text{DMSO}-d_6$) δ 1.44–1.80 (m, 6H), 2.06 (td, $J = 12.8, 4.3$ Hz, 2H), 2.29 (d, $J = 12.8$ Hz, 2H), 3.23 (t, $J = 13.9$ Hz, 2H), 3.59 (d, $J = 11.3$ Hz, 1H), 3.94 (d, $J = 8.5$ Hz, 2H), 4.09 (t, $J = 8.7$ Hz, 1H), 5.03 (s, 1H), 7.80 (dd, $J = 4.4, 1.6$ Hz, 2H), 8.00 (d, $J = 8.5$ Hz, 2H), 8.06 (d, $J = 8.8$ Hz, 2H), 8.13 (d, $J = 8.5$ Hz, 2H), 8.28 (d, $J = 8.8$ Hz, 2H), 8.68 (dd, $J = 4.4, 1.6$ Hz, 2H), 11.58 (s, 1H); ^{13}C NMR (75.4 MHz, $\text{DMSO}-d_6$) δ 17.8, 24.6, 27.3, 27.6, 61.2, 63.7, 69.6, 100.4, 119.9, 120.3, 120.9, 126.0, 127.4, 130.6, 132.1, 133.9, 136.9, 140.5, 146.2, 147.1, 150.2, 160.6; MS, m/z : 590.1 $[\text{M} + \text{H}]^+$.

4-((4-(4-(4-(Pyrimidin-5-yl)phenyl)-1H-1,2,3-triazol-1-yl)phenyl)sulfonyl)-N-((tetrahydro-2H-pyran-2-yl)oxy)tetrahydro-2H-pyran-4-carboxamide (3g). Following the general procedure for the preparation of triazoles **3a-i**, from 5-(4-ethynylphenyl)pyrimidine **4**, and using CH_2Cl_2 -MeOH (1.25% MeOH) as an eluent for chromatography, triazole **3g** (85 mg, 37%) was obtained as a white solid, mp 167–168 °C. IR (KBr): 3148, 2956, 1729, 1664 cm^{-1} ; ^1H NMR (300 MHz, CDCl_3) δ 1.60–1.72 (m, 3H), 1.75–1.90 (m, 3H), 2.14 (d, $J = 13.0$ Hz, 2H), 2.34 (td, $J = 12.4, 9.2$ Hz, 2H), 3.50 (t, $J = 12.2$ Hz, 2H), 3.73 (d, $J = 11.4$ Hz, 1H), 3.97–4.03 (m, 3H), 5.05 (s, 1H), 7.72 (d, $J = 8.3$ Hz, 2H), 8.05–8.11 (m, 6H), 8.39 (s, 1H), 9.03 (s, 2H), 9.24 (s, 1H), 9.60 (s, 1H); ^{13}C NMR (75.4 MHz, CDCl_3) δ 18.2, 24.9, 27.8, 28.2, 28.5, 62.5, 64.2, 64.3, 70.3, 102.9, 117.6, 120.4, 127.0, 127.6, 130.3, 132.2, 133.7, 133.9, 134.6, 141.2, 148.2, 154.8, 157.7, 163.6; MS, m/z : 591.1 $[\text{M} + \text{H}]^+$.

4-((4-(4-(6-(Piperidin-1-yl)pyridin-3-yl)-1H-1,2,3-triazol-1-yl)phenyl)sulfonyl)-N-((tetrahydro-2H-pyran-2-yl)oxy)tetrahydro-2H-pyran-4-carboxamide (3h). Following the general procedure for the preparation of triazoles **3a-i**, from 5-ethynyl-2-(piperidin-1-yl)pyridine,⁴⁰ and using CH_2Cl_2 -MeOH (1% MeOH) as an eluent for chromatography, triazole **3h** (162 mg, 70%) was obtained as a white solid, mp 173–174 °C (dec.). IR (KBr): 3323, 2940, 1688, 1615, 1595 cm^{-1} ; ^1H NMR (300 MHz, CDCl_3) δ 1.60–1.90 (m, 12H), 2.13 (d, $J = 13.0$ Hz, 2H), 2.32 (t, $J = 12.2$ Hz, 2H), 3.49 (td, $J = 11.9, 2.8$ Hz, 2H), 3.58–3.65 (m, 4H), 3.71 (d, $J = 11.5$ Hz, 1H), 3.95–4.10 (m, 3H), 5.04 (s, 1H), 6.74 (d, $J = 8.9$ Hz, 1H), 7.99–8.05 (m, 5H), 8.20 (s, 1H), 8.63 (d, $J = 2.1$ Hz, 1H), 9.55 (s, 1H); ^{13}C NMR (75.4 MHz, CDCl_3) δ 18.2, 24.7, 24.9, 25.5, 27.8, 28.3, 28.5, 46.2, 62.5, 64.2, 64.4, 70.2, 102.3, 106.7, 114.2, 115.6, 120.2, 132.1, 133.5, 135.1, 141.4, 145.8, 147.3, 159.4, 163.6; MS, m/z : 597.2 $[\text{M} + \text{H}]^+$.

4-((4-(4-(6-Morpholinopyridin-3-yl)-1H-1,2,3-triazol-1-yl)phenyl)sulfonyl)-N-((tetrahydro-2H-pyran-2-yl)oxy)tetrahydro-

2H-pyran-4-carboxamide (3i). Following the general procedure for the preparation of triazoles **3a-i**, from 4-(5-ethynylpyridin-2-yl)morpholine,⁴¹ and using CH_2Cl_2 -MeOH (1.25% MeOH) as an eluent for chromatography, triazole **3i** (182 mg, 78%) was obtained as a white solid, mp 168–169 °C (dec.). IR (KBr): 3164, 2960, 1688, 1676 cm^{-1} ; ^1H NMR (300 MHz, CDCl_3) δ 1.60–1.72 (m, 3H), 1.75–1.92 (m, 3H), 2.11 (d, $J = 13.0$ Hz, 2H), 2.34 (td, $J = 12.8, 4.7$ Hz, 2H), 3.51 (td, $J = 11.9, 2.8$ Hz, 2H), 3.58–3.66 (m, 4H), 3.75 (d, $J = 11.8$ Hz, 1H), 3.79–3.91 (m, 4H), 3.96–4.05 (m, 3H), 5.04 (s, 1H), 6.76 (d, $J = 8.8$ Hz, 1H), 7.97–8.13 (m, 5H), 8.20 (s, 1H), 8.66 (d, $J = 2.1$ Hz, 1H), 9.41 (s, 1H); ^{13}C NMR (75.4 MHz, CDCl_3) δ 18.2, 24.9, 27.8, 28.2, 28.5, 45.5, 62.5, 64.2, 64.4, 66.7, 70.3, 102.0, 106.7, 115.7, 115.8, 120.3, 132.2, 133.6, 135.3, 141.3, 145.7, 147.0, 159.4, 163.7; MS, m/z : 599.2 $[\text{M} + \text{H}]^+$.

General procedure for hydrochloride salt preparation

A suspension of the corresponding triazole (1.00 eq.) in 4 M HCl dioxane solution (2–4 mL) and methanol (a drop) was stirred at rt under argon for 20 minutes. Et_2O was added and the precipitate was filtered, washed with Et_2O , CH_2Cl_2 and dried.

4-((4-(4-(4-(Dimethylamino)phenyl)-1H-1,2,3-triazol-1-yl)phenyl)sulfonyl)-N-hydroxytetrahydro-2H-pyran-4-carboxamide hydrochloride (1e). From **3e** (72 mg, 0.13 mmol), triazole **1e** (62 mg, 94%) was obtained as a yellowish solid, mp 205–206 °C (dec.). IR (KBr): 3107, 2870, 1676, 1631 cm^{-1} ; ^1H NMR (300 MHz, $\text{DMSO}-d_6$) δ 1.99 (td, $J = 13.0, 4.3$ Hz, 2H), 2.27 (d, $J = 13.0$ Hz, 2H), 3.07 (s, 6H), 3.18 (t, $J = 11.7$ Hz, 2H), 3.91 (dd, $J = 11.7, 3.4$ Hz, 2H), 7.10 (br s, 2H), 7.87 (d, $J = 8.5$ Hz, 2H), 7.98 (d, $J = 8.7$ Hz, 2H), 8.24 (d, $J = 8.7$ Hz, 2H), 9.39 (s, 1H), 11.09 (br s, 1H); ^{13}C NMR (75.4 MHz, $\text{DMSO}-d_6$) δ 27.2, 42.3, 63.8, 69.5, 116.4, 119.0, 119.2, 119.8, 126.5, 127.1, 132.2, 133.8, 140.5, 147.6, 160.3; MS, m/z : 472.1 $[\text{M} + \text{H}]^+$; Anal. calcd for $\text{C}_{22}\text{H}_{26}\text{ClN}_5\text{O}_5\text{S} + 0.5\text{H}_2\text{O}$: C, 51.11; H, 5.26; N, 13.55; S, 6.20. Found: C, 51.38; H, 5.21; N, 13.47; S, 6.12.

N-Hydroxy-4-((4-(4-(pyridin-4-yl)phenyl)-1H-1,2,3-triazol-1-yl)phenyl)sulfonyl)tetrahydro-2H-pyran-4-carboxamide hydrochloride (1f). From **3f** (28 mg, 0.05 mmol), triazole **1f** (23 mg, 88%) was obtained as a white solid, mp 247–248 °C (dec.). IR (KBr): 3376, 3107, 1660, 1635 cm^{-1} ; ^1H NMR (300 MHz, $\text{DMSO}-d_6$) δ 2.00 (td, $J = 12.8, 4.0$ Hz, 2H), 2.27 (d, $J = 12.8$ Hz, 2H), 3.18 (t, $J = 11.6$ Hz, 2H), 3.91 (dd, $J = 11.6, 3.1$ Hz, 2H), 8.01 (d, $J = 8.7$ Hz, 2H), 8.22 (s, 4H), 8.27 (d, $J = 8.7$ Hz, 2H), 8.40 (d, $J = 6.4$ Hz, 2H), 8.95 (d, $J = 6.0$ Hz, 2H), 9.75 (s, 1H), 11.11 (br s, 1H); ^{13}C NMR (100 MHz, $\text{DMSO}-d_6$) δ 27.2, 63.8, 69.5, 120.0, 121.1, 123.2, 126.3, 128.7, 132.2, 132.6, 134.1, 134.4, 140.4, 143.6, 146.7, 153.3, 160.4; MS, m/z : 506.1 $[\text{M} + \text{H}]^+$; Anal. calcd for $\text{C}_{25}\text{H}_{24}\text{ClN}_5\text{O}_5\text{S} + 1.8\text{H}_2\text{O}$: C, 52.27; H, 4.84; N, 12.19; S, 5.58. Found: C, 52.37; H, 4.88; N, 12.08; S, 5.38.

N-Hydroxy-4-((4-(4-(pyrimidin-5-yl)phenyl)-1H-1,2,3-triazol-1-yl)phenyl)sulfonyl)tetrahydro-2H-pyran-4-carboxamide hydrochloride (1g). From **3g** (31 mg, 0.053 mmol), triazole **1g** (28 mg, 98%) was obtained as a white solid, mp 226–227 °C (dec.). IR (KBr): 3388, 3107, 1664 cm^{-1} ; ^1H NMR (300 MHz, $\text{DMSO}-d_6$) δ 1.90–2.08 (m, 2H), 2.27 (d, $J = 13.0$ Hz,

2H), 3.18 (t, $J = 11.6$ Hz, 2H), 3.91 (d, $J = 9.9$ Hz, 2H), 7.95–8.05 (m, 4H), 8.14 (d, $J = 8.0$ Hz, 2H), 8.27 (d, $J = 8.3$ Hz, 2H), 9.19–9.27 (m, 3H), 9.66 (s, 1H), 11.10 (br s, 1H); ^{13}C NMR (75.4 MHz, DMSO- d_6) δ 27.2, 63.8, 69.5, 119.8, 119.9, 120.4, 126.2, 127.6, 130.3, 131.2, 132.6, 133.6, 134.1, 140.4, 147.1, 154.6, 157.3; MS, m/z : 507.1 $[\text{M} + \text{H}]^+$; Anal. calcd for $\text{C}_{24}\text{H}_{23}\text{ClN}_6\text{O}_5\text{S} + 1.5\text{H}_2\text{O}$: C, 50.57; H, 4.60; N, 14.74; S, 5.44. Found: C, 50.72; H, 4.61; N, 14.54; S, 5.44.

N-Hydroxy-4-((4-(4-(6-(piperidin-1-yl)pyridin-3-yl)-1H-1,2,3-triazol-1-yl)phenyl)sulfonyl)tetrahydro-2H-pyran-4-carboxamide hydrochloride (1h). From **3h** (125 mg, 0.21 mmol), triazole **1h** (110 mg, 96%) was obtained as a white solid, mp 260–261 °C (dec.). IR (KBr): 3152, 1660, 1615, 1599 cm^{-1} ; ^1H NMR (300 MHz, DMSO- d_6) δ 1.6–1.72 (m, 6H), 1.99 (td, $J = 12.8$, 4.4 Hz, 2H), 2.26 (d, $J = 12.9$ Hz, 2H), 3.18 (t, $J = 11.6$ Hz, 2H), 3.73–3.79 (m, 4H), 3.91 (dd, $J = 11.4$, 2.4 Hz, 2H), 7.49 (d, $J = 9.6$ Hz, 1H), 8.00 (d, $J = 8.8$ Hz, 2H), 8.22 (d, $J = 8.8$ Hz, 2H), 8.35 (d, $J = 8.4$ Hz, 1H), 8.50 (d, $J = 2.0$ Hz, 1H), 9.62 (s, 1H), 11.09 (br s, 1H); ^{13}C NMR (75.4 MHz, DMSO- d_6) δ 23.7, 25.3, 27.6, 47.6, 64.2, 69.9, 112.8, 115.0, 120.2, 120.3, 132.6, 134.5, 135.2, 139.6, 140.6, 143.8, 152.5, 160.6; MS, m/z : 513.1 $[\text{M} + \text{H}]^+$; Anal. calcd for $\text{C}_{24}\text{H}_{29}\text{ClN}_6\text{O}_5\text{S} + 0.8\text{H}_2\text{O}$: C, 51.16; H, 5.47; N, 14.92; S, 5.69. Found: C, 51.66; H, 5.34; N, 14.61; S, 5.48.

N-Hydroxy-4-((4-(4-(6-morpholinopyridin-3-yl)-1H-1,2,3-triazol-1-yl)phenyl)sulfonyl)tetrahydro-2H-pyran-4-carboxamide hydrochloride (1i). From **3i** (126 mg, 0.21 mmol), triazole **1i** (112 mg, 97%) was obtained as a white solid, mp 249–250 °C (dec.). IR (KBr): 3441, 3144, 1656, 1615 cm^{-1} ; ^1H NMR (300 MHz, DMSO- d_6) δ 2.00 (td, $J = 12.8$, 4.4 Hz, 2H), 2.26 (d, $J = 12.9$ Hz, 2H), 3.17 (t, $J = 11.6$ Hz, 2H), 3.60–3.67 (m, 4H), 3.73–3.78 (m, 4H), 3.91 (dd, $J = 11.4$, 3.4 Hz, 2H), 7.26 (d, $J = 9.2$ Hz, 1H), 7.99 (d, $J = 8.8$ Hz, 2H), 8.18–8.30 (m, 3H), 8.35 (d, $J = 8.4$ Hz, 1H), 8.64 (d, $J = 2.1$ Hz, 1H), 9.53 (s, 1H), 11.10 (br s, 1H); ^{13}C NMR (75.4 MHz, DMSO- d_6) δ 27.2, 45.8, 63.9, 65.5, 69.5, 110.6, 115.7, 119.7, 119.9, 132.3, 134.1, 137.8, 138.3, 140.4, 144.2, 154.9, 160.3; MS, m/z : 515.1 $[\text{M} + \text{H}]^+$; Anal. calcd for $\text{C}_{23}\text{H}_{27}\text{ClN}_6\text{O}_6\text{S} + 0.4\text{H}_2\text{O}$: C, 49.49; H, 5.02; N, 15.05; S, 5.74. Found: C, 49.53; H, 4.99; N, 14.81; S, 5.53.

5-(4-Ethynylphenyl)pyrimidine (4). 4-(Pyrimidin-5-yl)benzaldehyde (0.5 g, 2.73 mmol) was dissolved in anhydrous MeOH (25 mL) and stirred under argon at rt. Anhydrous K_2CO_3 (1.13 g, 8.19 mmol) and Bestmann–Ohira reagent¹³ (1.05 g, 5.46 mmol) were added to the reaction mixture and stirring was continued for 24 h at rt. The solvent was evaporated, and the remaining residue was dissolved in EtOAc and washed with saturated NH_4Cl aq. solution and water. The organic layer was dried over Na_2SO_4 , filtered off and concentrated *in vacuo*. The crude product was purified by flash chromatography (silica gel, 7 : 3 hexane–EtOAc) to give 465 mg (95%) of **4** as a white solid, mp 147–149 °C. IR (KBr): 3254, 3221, 1570, 1549 cm^{-1} ; ^1H NMR (300 MHz, CDCl_3) δ 3.19 (1H, s), 7.56 (d, $J = 8.5$ Hz, 2H), 7.65 (d, $J = 8.5$ Hz, 2H), 8.95 (s, 2H), 9.22 (s, 1H); ^{13}C NMR (CDCl_3 , 100 MHz) δ 79.1, 82.8, 123.1, 126.9, 133.2, 133.6, 134.6, 154.9, 157.8. MS, m/z : 180.90 $[\text{M} + \text{H}]^+$.

1-tert-Butyl 4-ethyl 4-((4-nitrophenyl)sulfonyl)piperidine-1,4-dicarboxylate (6). To a solution of 1-tert-butyl 4-ethyl piperidine-1,4-dicarboxylate **5**⁵ (8.15 g, 31.7 mmol) in dry THF (100 mL) was slowly transferred to a freshly prepared 1 M solution of LDA in dry THF (33.3 mL, 33.3 mmol) at -78 °C, under argon. The resulting mixture was allowed to slowly reach 0 °C over 1 h. Commercially available 4-nitrophenyl disulfide (10.3 g, 33.3 mmol) was added at 0 °C and the resulting brown suspension was stirred at 0 °C for 2 h and overnight at rt, under argon. The reaction was quenched with water at 0 °C. The reaction mixture was concentrated, water was added and the product was extracted with EtOAc (2×150 mL). The organic layers were combined, washed with water and brine, dried over anhydrous MgSO_4 , filtered and evaporated to give 13.9 g of brown oil. The crude product was purified by column chromatography (9 : 1 hexane–EtOAc) to afford **6** (9.70 g, 74%) as an orange oil. ^1H NMR (300 MHz, CDCl_3) δ 1.24 (t, $J = 7.1$ Hz, 3H), 1.45 (s, 9H), 1.79–1.85 (m, 2H), 2.12–2.17 (m, 2H), 3.10–3.18 (m, 2H), 3.75–3.79 (br s, 2H), 4.18 (q, $J = 7.1$ Hz, 2H), 7.60 (d, $J = 8.8$ Hz, 2H), 8.17 (d, $J = 8.8$ Hz, 2H); ^{13}C NMR (75.4 MHz, CDCl_3) δ 14.2, 28.5, 33.4, 40.9 (br), 54.5, 61.8, 80.1, 123.7, 136.5, 139.1, 148.3, 154.7, 171.6; MS, m/z : 433.1 $[\text{M} + \text{Na}]^+$; Anal. calcd for $\text{C}_{19}\text{H}_{26}\text{N}_2\text{O}_6\text{S}$: C, 55.60; H, 6.38; N, 6.82; S, 7.81. Found: C, 55.70; H, 6.52; N, 6.65; S, 7.58.

1-(tert-Butoxycarbonyl)-4-(4-nitrophenylthio)piperidine-4-carboxylic acid (7). To a solution of ethyl ester **6** (9.60 g, 23.4 mmol) in EtOH (96%, 100 mL) was added a freshly prepared 2 N aq. NaOH solution (58 mL, 117 mmol) and the reaction mixture was stirred at rt for 2 days. After evaporating most of the ethanol in a rotary evaporator, the resulting solution was washed with CH_2Cl_2 (3×20 mL), acidified to pH = 2–3 with 6 N HCl and extracted with EtOAc. The organic layer was washed with brine, dried over anhydrous MgSO_4 , filtered and evaporated to give **7** (8.33 g, 93%) as a yellow solid, mp 152–153 °C. IR (KBr): 2967, 1719 cm^{-1} ; ^1H NMR (300 MHz, CDCl_3) δ 1.45 (s, 9H), 1.78–1.85 (m, 2H), 2.09–2.15 (m, 2H), 3.18–3.24 (m, 2H), 3.75–3.79 (m, 2H), 7.64 (d, $J = 8.5$ Hz, 2H), 8.15 (d, $J = 8.5$ Hz, 2H), 9.94 (br s, 1H); ^{13}C NMR (75.4 MHz, CDCl_3) δ 28.5, 33.0, 40.9 (br s), 54.2, 80.7, 123.8, 136.6, 138.6, 148.4, 154.9, 176.1; MS, m/z : 405.1 $[\text{M} + \text{Na}]^+$; Anal. calcd for $\text{C}_{17}\text{H}_{22}\text{N}_2\text{O}_6\text{S}$: C, 53.39; H, 5.80; N, 7.33; S, 8.38. Found: C, 53.41; H, 5.73; N, 7.28; S, 8.35.

1-(tert-Butoxycarbonyl)-4-(4-nitrophenylsulfonyl)piperidine-4-carboxylic acid (8). To a suspension of carboxylic acid **7** (3.21 g, 8.39 mmol) in dry CH_2Cl_2 (100 mL) was added MCPBA (4.35 g, 25.2 mmol) at 0 °C. The resulting mixture was stirred at 0 °C for 1 h and overnight at rt. The solvent was evaporated and the resulting solid was suspended in Et_2O , filtered, washed with Et_2O , dried and recrystallized from hexane–EtOAc to give **8** (2.70 g, 78%) as a white solid, mp 176–177 °C. IR (KBr): 2974, 1717 cm^{-1} ; ^1H NMR (300 MHz, DMSO- d_6) δ 1.39 (s, 9H), 1.82–1.88 (m, 2H), 2.15 (d, $J = 12.8$ Hz, 2H), 2.63 (br s, 2H), 4.02–4.06 (m, 2H), 8.08 (d, $J = 8.9$ Hz, 2H), 8.45 (d, $J = 8.9$ Hz, 2H); ^{13}C NMR (75.4 MHz, DMSO- d_6) δ 27.2, 28.0, 72.2, 79.3, 124.2, 132.0, 140.1, 151.0, 153.6, 167.2; MS, m/z : 437.1 $[\text{M} + \text{Na}]^+$; Anal. calcd for $\text{C}_{17}\text{H}_{22}\text{N}_2\text{O}_8\text{S}$: C,

49.27; H, 5.35; N, 6.76; S, 7.74. Found: C, 48.89; H, 5.32; N, 6.99; S, 7.45.

4-(4-Aminophenylsulfonyl)-1-(*tert*-butoxycarbonyl)piperidine-4-carboxylic acid (9). A suspension of **8** (2.60 g, 6.27 mmol) and black Pd (52 mg, 2 mol.%) in absolute EtOH (100 mL) was stirred at rt in a Parr Shaker apparatus, under 60 p.s.i. (4.14 bar) of H₂ for 3 days. The reaction mixture was filtered on celite® 545, washed with 5% MeOH in EtOAc and evaporated to afford **9** (2.40 g, 99%) as an orange foam, mp 187–189 °C. IR (KBr): 3462, 3382, 2984, 1722, 1632 cm⁻¹; ¹H NMR (300 MHz, DMSO-*d*₆) δ 1.37 (s, 9H), 1.60–1.70 (m, 2H), 2.14 (d, *J* = 12.8 Hz, 2H), 2.57 (br s, 2H), 3.96–4.01 (m, 2H), 6.27 (br s, 2H), 6.61 (d, *J* = 8.8 Hz, 2H), 7.34 (d, *J* = 8.8 Hz, 2H); ¹³C NMR (75.4 MHz, DMSO-*d*₆) δ 27.7, 28.0, 71.2, 79.1, 112.4, 118.6, 132.0, 153.7, 154.4, 167.9; MS, *m/z*: 407.0 [M + Na]⁺.

4-(4-Azidophenylsulfonyl)-1-(*tert*-butoxycarbonyl)piperidine-4-carboxylic acid (10). Carboxylic acid **9** (2.30 g, 5.98 mmol) was suspended in dry MeCN (50 mL), and *t*BuONO (1.07 mL, 9.00 mmol) followed by TMSN₃ (0.96 mL, 7.20 mmol, 5 minutes later) were slowly added at 0 °C, under argon. The resulting mixture was stirred at 0 °C for 30 minutes and then at rt for 2 h. The reaction mixture was partitioned between water and EtOAc. The organic layer was washed with water and brine, dried over anhydrous MgSO₄, filtered and evaporated to give 2.6 g of a brown solid. The crude product was purified by column chromatography (99.5 : 0.5 to 98.5/1.5 CH₂Cl₂–MeOH) to afford **10** (1.72 g, 70%) as an orange solid, mp 168–169 °C. IR (KBr): 2977, 2559, 2119, 1720, 1615 cm⁻¹; ¹H NMR (300 MHz, DMSO-*d*₆) δ 1.38 (s, 9H), 1.71–1.81 (m, 2H), 2.14 (d, *J* = 12.7 Hz, 2H), 2.61 (br s, 2H), 4.00–4.04 (m, 2H), 7.36 (d, *J* = 8.7 Hz, 2H), 7.78 (d, *J* = 8.7 Hz, 2H); ¹³C NMR (75.4 MHz, DMSO-*d*₆) δ 27.4, 28.0, 71.7, 79.2, 119.6, 130.5, 132.2, 146.0, 153.7, 167.4; MS, *m/z*: 433.0 [M + Na]⁺.

***tert*-Butyl-4-(4-azidophenylsulfonyl)-4-(tetrahydro-2H-pyran-2-yloxy)carbamoyl)piperidine-1-carboxylate (11).** To a solution of **10** (1.60 g, 3.90 mmol) in DMF (40 mL) were added HOBt hydrate (632 mg, 4.68 mmol), EDCI (1.05 g, 5.46 mmol) and NMM (1.10 mL, 15.6 mmol). The resulting mixture was stirred for 10 min at rt and *O*-tetrahydro-2H-pyran-2-yl-hydroxylamine (914 mg, 7.80 mmol) was added. The reaction mixture was stirred overnight at rt. Water was added and the product was extracted with EtOAc (3 × 40 mL). The organic layers were combined, washed with saturated NH₄Cl solution, water and brine, dried over anhydrous MgSO₄, filtered and evaporated to give 2.8 g of a brown oil, which was purified by column chromatography (99.5 : 0.5 CH₂Cl₂–MeOH) to afford **11** (953 mg, 48%) as a yellow solid, mp 132–133 °C. IR (KBr): 3306, 2844, 2132, 1694 cm⁻¹; ¹H NMR (300 MHz, CDCl₃) δ 1.45 (s, 9H), 1.60–1.67 (m, 3H), 1.72–1.89 (m, 3H), 2.08–2.16 (m, 4H), 2.85 (br s, 2H), 3.69–3.73 (m, 1H), 3.97–4.04 (m, 1H), 4.16 (br s, 2H), 5.00 (s, 1H), 7.17 (d, *J* = 8.7 Hz, 2H), 7.83 (d, *J* = 8.7 Hz, 2H), 9.43 (s, 1H); ¹³C NMR (75.4 MHz, CDCl₃) δ 18.2, 24.9, 27.8, 28.1, 28.4, 38.8 (br), 62.4, 70.9, 80.2, 102.0, 119.6, 129.7, 132.0, 147.1, 154.4, 163.8; MS, *m/z*: 532.1 [M + Na]⁺; Anal. calcd for C₂₂H₃₁N₅O₇S: C, 51.85; H, 6.13; N, 13.74; S, 6.29. Found: C, 51.92; H, 6.26; N, 12.98; S, 5.99.

General procedure for the preparation of triazoles 12a–j

A mixture of **11** (100 mg, 0.20 mmol, 1.00 eq.), the corresponding alkyne (0.26 mmol, 1.30 eq.), freshly prepared aqueous 0.1 M CuSO₄·5H₂O solution (118 μL, 0.01 mmol, 0.06 eq.) and 0.5 M sodium ascorbate solution (78 μL, 0.04 mmol, 0.20 eq.) in DMF (1–3 mL) was stirred at rt under argon for 16–24 h. The reaction mixture was partitioned between CH₂Cl₂ and water. The organic layer was washed with 15% aqueous ammonia, water and brine, dried over anhydrous MgSO₄, filtered and evaporated. The crude product was purified by column chromatography on silica gel.

***tert*-Butyl-4-(4-(4-(biphenyl-4-yl)-1H-1,2,3-triazol-1-yl)phenylsulfonyl)-4-(tetrahydro-2H-pyran-2-yloxy)carbamoyl)piperidine-1-carboxylate (12a).** Following the general procedure for the preparation of triazoles 12a–j, from commercially available 4-ethynyl-1,1'-biphenyl, and using 7 : 3 hexane–EtOAc as an eluent for chromatography, triazole **12a** (78 mg, 58%) was obtained as a white solid, mp 203–204 °C. IR (KBr): 3313, 2940, 1694 cm⁻¹; ¹H NMR (300 MHz, CDCl₃) δ 1.44 (s, 9H), 1.63 (“br s”, 3H), 1.78–1.87 (m, 3H), 2.14–2.23 (m, 4H), 2.86 (br s, 2H), 3.69–3.73 (m, 1H), 3.99–4.06 (m, 1H), 4.22 (br s, 2H), 5.04 (s, 1H), 7.37 (“d”, 1H), 7.45 (t, *J* = 7.6 Hz, 2H), 7.63 (d, *J* = 7.1 Hz, 2H), 7.69 (d, *J* = 8.2 Hz, 2H), 7.97 (d, *J* = 8.2 Hz, 2H), 8.04 (s, 4H), 8.33 (s, 1H), 9.57 (s, 1H); ¹³C NMR (75.4 MHz, CDCl₃) δ 18.3, 25.0, 27.9, 28.1, 28.4, 40.0–40.8, 62.5, 71.2, 80.4, 102.1, 117.3, 120.3, 126.4, 127.1, 127.8, 128.5, 129.0, 132.2, 133.7, 140.4, 141.4, 141.7, 148.9, 154.4, 163.4; MS, *m/z*: 710.3 [M + Na]⁺, 726.2 [M + K]⁺.

***tert*-Butyl-4-(4-(4-(4-pentylphenyl)-1H-1,2,3-triazol-1-yl)phenylsulfonyl)-4-(tetrahydro-2H-pyran-2-yloxy)carbamoyl)piperidine-1-carboxylate (12b).** Following the general procedure for the preparation of triazoles 12a–j, from commercially available 1-ethynyl-4-pentylbenzene, and using 3 : 2 hexane–EtOAc as an eluent for chromatography, triazole **12b** (53 mg, 39%) was obtained as a yellow solid, mp 106–107 °C. IR (KBr): 3299, 2930, 2856, 1694 cm⁻¹; ¹H NMR (300 MHz, CDCl₃) δ 0.82 (t, *J* = 6.8 Hz, 3H), 1.24–1.29 (m, 4H), 1.37 (s, 9H), 1.52–1.60 (m, 5H), 1.70–1.79 (m, 3H), 2.04–2.16 (m, 4H), 2.57 (t, *J* = 7.5 Hz, 2H), 2.79 (br s, 2H), 3.60–3.64 (m, 1H), 3.91–3.98 (m, 1H), 4.12 (br s, 2H), 4.96 (s, 1H), 7.20 (d, *J* = 8.2 Hz, 2H), 7.73 (d, *J* = 8.2 Hz, 2H), 7.95 (s, 4H), 8.20 (s, 1H), 9.51 (s, 1H); ¹³C NMR (75.4 MHz, CDCl₃) δ 14.1, 18.3, 22.6, 25.0, 27.9, 28.1, 28.4, 31.1, 31.5, 35.8, 40.5 (br), 62.5, 71.2, 80.3, 102.1, 116.9, 120.3, 126.0, 127.0, 129.1, 132.2, 133.7, 141.4, 144.0, 149.3, 154.4, 163.4; MS, *m/z*: 704.3 [M + Na]⁺.

***tert*-Butyl-4-(((4-(4-(4-methoxyphenyl)-1H-1,2,3-triazol-1-yl)phenyl)sulfonyl)-4-(((tetrahydro-2H-pyran-2-yl)oxy)carbamoyl)piperidine-1-carboxylate (12c).** Following the general procedure for the preparation of triazoles 12a–j, from commercially available 1-ethynyl-4-methoxybenzene, and using 1.25% MeOH in CH₂Cl₂ as an eluent for chromatography, triazole **12c** (88 mg, 70%) was obtained as a beige solid, mp 136–137 °C. IR (KBr): 3311, 2938, 1694 cm⁻¹; ¹H NMR (300 MHz, CDCl₃) δ 1.45 (s, 9H), 1.61–1.72 (m, 3H), 1.78–1.90 (m, 3H), 2.17 (br s, 4H), 2.85 (br s, 2H), 3.72–3.76 (m, 1H), 3.87 (s, 3H), 3.99–4.06

(m, 1H), 4.19 (br s, 2H), 5.03 (s, 1H), 7.02 (d, $J = 8.8$ Hz, 2H), 7.85 (d, $J = 8.8$ Hz, 2H), 8.05 (s, 4H), 8.19 (s, 1H), 9.40 (s, 1H); ^{13}C NMR (75.4 MHz, CDCl_3) δ 18.3, 25.0, 27.9, 28.1, 28.4, 40.2 (br), 55.4, 62.5, 71.2, 80.3, 102.1, 114.5, 116.4, 120.2, 122.2, 127.4, 132.2, 133.6, 141.4, 149.1, 154.4, 160.2, 163.4; MS, m/z : 664.3 $[\text{M} + \text{Na}]^+$.

tert-Butyl 4-((4-(4-phenoxyphenyl)-1H-1,2,3-triazol-1-yl)phenyl)sulfonyl-4-(((tetrahydro-2H-pyran-2-yl)oxy)carbamoyl)piperidine-1-carboxylate (12d). Following the general procedure for the preparation of triazoles **12a–j**, from commercially available 1-ethynyl-4-phenoxybenzene, and using 6:4 hexane–EtOAc as an eluent for chromatography, triazole **12d** (80 mg, 58%) was obtained after recrystallization from hexane–EtOAc, as a white solid, mp 127–128 °C. IR (KBr): 3290, 2957, 1694 cm^{-1} ; ^1H NMR (300 MHz, CDCl_3) δ 1.45 (s, 9H), 1.65 (br s, 3H), 1.78–1.89 (m, 3H), 2.17 (br s, 4H), 2.88 (br s, 2H), 3.71–3.75 (m, 1H), 3.99–4.05 (m, 1H), 4.20 (br s, 2H), 5.03 (s, 1H), 7.05–7.18 (m, 5H), 7.35–7.40 (m, 2H), 7.87 (d, $J = 8.7$ Hz, 2H), 8.05 (s, 4H), 8.23 (s, 1H), 9.42 (s, 1H); ^{13}C NMR (75.4 MHz, CDCl_3) δ 18.3, 25.0, 27.9, 28.2, 28.5, 40.9 (br), 62.6, 71.2, 80.4, 102.1, 116.7, 119.2, 119.4, 120.4, 123.9, 124.6, 127.6, 130.0, 132.3, 133.8, 141.5, 148.9, 154.5, 156.8, 158.2, 163.6; MS, m/z : 726.2 $[\text{M} + \text{Na}]^+$.

tert-Butyl 4-((4-(4-(dimethylamino)phenyl)-1H-1,2,3-triazol-1-yl)phenyl)sulfonyl-4-(((tetrahydro-2H-pyran-2-yl)oxy)carbamoyl)piperidine-1-carboxylate (12e). Following the general procedure for the preparation of triazoles **12a–j**, from commercially available 4-ethynyl-*N,N*-dimethylaniline, and using 8:2 hexane–EtOAc as an eluent for chromatography, triazole **12e** (77 mg, 60%) was obtained as a pale yellow solid, mp 153–154 °C. IR (KBr): 3321, 2937, 1694, 1502 cm^{-1} ; ^1H NMR (300 MHz, CDCl_3) δ 1.45 (s, 9H), 1.62–1.70 (m, 3H), 1.79–1.90 (m, 3H), 2.17 (br s, 4H), 2.87 (br s, 2H), 3.03 (s, 6H), 3.72–3.76 (m, 1H), 3.99–4.5 (m, 1H), 4.19 (br s, 2H), 5.03 (s, 1H), 6.81 (d, $J = 8.8$ Hz, 2H), 7.78 (d, $J = 8.8$ Hz, 2H), 8.04 (s, 4H), 8.13 (s, 1H), 9.39 (s, 1H); ^{13}C NMR (75.4 MHz, CDCl_3) δ 18.3, 25.0, 27.9, 28.2, 28.5, 40.5 (two signals), 62.6, 71.2, 80.4, 102.1, 112.5, 115.4, 117.5, 120.2, 127.1, 132.2, 133.4, 141.7, 149.8, 150.9, 154.5, 163.6; MS, m/z : 655.3 $[\text{M} + \text{H}]^+$, 677.3 $[\text{M} + \text{Na}]^+$; Anal. calcd for $\text{C}_{32}\text{H}_{42}\text{N}_6\text{O}_7\text{S}$: C, 58.70; H, 6.47; N, 12.83; S, 4.90. Found: C, 58.28; H, 6.51; N, 12.46; S, 4.74.

tert-Butyl 4-((4-(4-(4-fluorophenyl)-1H-1,2,3-triazol-1-yl)phenyl)sulfonyl-4-(((tetrahydro-2H-pyran-2-yl)oxy)carbamoyl)piperidine-1-carboxylate (12f). Following the general procedure for the preparation of triazoles **12a–j**, from commercially available 1-ethynyl-4-fluorobenzene, and using 7:3 hexane–EtOAc as an eluent for chromatography, triazole **12f** (86 mg, 70%) was obtained as a yellow solid, mp 132–133 °C. IR (KBr): 3268, 2934, 1695 cm^{-1} ; ^1H NMR (400 MHz, CDCl_3) δ 1.44 (s, 9H), 1.60–1.63 (m, 3H), 1.78–1.87 (m, 3H), 2.14–2.20 (m, 4H), 2.87 (br s, 2H), 3.70–3.72 (m, 1H), 3.99–4.04 (m, 1H), 4.18 (br s, 2H), 5.03 (s, 1H), 7.16 (t, $J = 8.5$ Hz, 2H), 7.88 (dd, $J = 8.5, 5.3$ Hz, 2H), 8.03 (s, 4H), 8.25 (s, 1H), 9.46 (br s, 1H); ^{13}C NMR (100 MHz, CDCl_3) δ 18.3, 25.0, 27.9, 28.1, 28.5, 40.7 (br), 62.6, 71.2, 80.4, 102.2, 116.2 (d, $^2J_{\text{CF}} = 21.8$ Hz), 117.1, 120.4, 125.9 (d, $^4J_{\text{CF}} = 3.1$ Hz), 127.8 (d,

$^3J_{\text{CF}} = 8.1$ Hz), 132.3, 133.9, 141.4, 148.4, 154.5, 163.2 (d, $^1J_{\text{CF}} = 247.0$ Hz), 163.5; MS, m/z : 652.2 $[\text{M} + \text{Na}]^+$.

tert-Butyl 4-((4-(4-(3-fluorophenyl)-1H-1,2,3-triazol-1-yl)phenyl)sulfonyl-4-(((tetrahydro-2H-pyran-2-yl)oxy)carbamoyl)piperidine-1-carboxylate (12g). Following the general procedure for the preparation of triazoles **12a–j**, from commercially available 1-ethynyl-3-fluorobenzene and using 7:3 hexane–EtOAc as an eluent for chromatography, triazole **12g** (79 mg, 64%) was obtained as an orange solid, mp 146–147 °C. IR (KBr): 3282, 2946, 1694 cm^{-1} ; ^1H NMR (300 MHz, CDCl_3) δ 1.45 (s, 9H), 1.66–1.71 (m, 3H), 1.77–1.90 (m, 3H), 2.17 (br s, 4H), 2.86 (br s, 2H), 3.71–3.75 (m, 1H), 3.99–4.05 (m, 1H), 4.18 (br s, 2H), 5.03 (s, 1H), 7.10 (td, $J = 8.5, 1.9$ Hz, 1H), 7.45 (“q”, $J = 7.9$ Hz, 1H), 7.63–7.67 (m, 2H), 8.06 (s, 4H), 8.30 (s, 1H), 9.41 (s, 1H); ^{13}C NMR (75.4 MHz, CDCl_3) δ 18.3, 25.0, 27.9, 28.1, 28.5, 39.8 (br s), 62.6, 71.2, 80.4, 102.2, 113.1 (d, $^2J_{\text{CF}} = 23.1$ Hz), 115.9 (d, $^2J_{\text{CF}} = 21.6$ Hz), 117.8, 120.5, 121.7 (d, $^4J_{\text{CF}} = 3.0$ Hz), 130.8 (d, $^3J_{\text{CF}} = 8.2$ Hz), 131.8 (d, $^3J_{\text{CF}} = 8.5$ Hz), 132.3, 134.1, 141.3, 148.2, 154.5, 163.2 (d, $^1J_{\text{CF}} = 256.1$ Hz), 163.5; MS, m/z : 652.2 $[\text{M} + \text{Na}]^+$.

tert-Butyl 4-((4-(4-(2-fluorophenyl)-1H-1,2,3-triazol-1-yl)phenyl)sulfonyl-4-(((tetrahydro-2H-pyran-2-yl)oxy)carbamoyl)piperidine-1-carboxylate (12h). Following the general procedure for the preparation of triazoles **12a–j**, from commercially available 1-ethynyl-2-fluorobenzene and using 7:3 hexane–EtOAc as an eluent for chromatography, triazole **12h** (82 mg, 66%) was obtained as a pale yellow solid, mp 132–134 °C. IR (KBr): 3274, 2956, 1695 cm^{-1} ; ^1H NMR (400 MHz, CDCl_3) δ 1.46 (s, 9H), 1.61–1.64 (m, 3H), 1.80–1.89 (m, 3H), 2.14–2.23 (m, 4H), 2.87 (br s, 2H), 3.70–3.73 (m, 1H), 4.01–4.09 (m, 1H), 4.19 (br s, 2H), 5.05 (s, 1H), 7.19 (dd, $J = 10.9, 8.1$ Hz, 1H), 7.30 (t, $J = 7.5$ Hz, 1H), 7.35–7.40 (m, 1H), 8.06 (s, 4H), 8.37 (td, $J = 7.5, 1.6$ Hz, 1H), 8.46 (d, $J = 3.1$ Hz, 1H), 9.54 (s, 1H); ^{13}C NMR (100 MHz, CDCl_3) δ 18.3, 25.0, 27.9, 28.1, 28.4, 40.9 (br), 62.5, 71.2, 80.3, 102.1, 116.9 (d, $^2J_{\text{CF}} = 21.6$ Hz), 117.7 (d, $^3J_{\text{CF}} = 12.5$ Hz), 120.3, 120.4, 124.9 (d, $^3J_{\text{CF}} = 9.1$ Hz), 128.1 (d, $^4J_{\text{CF}} = 3.1$ Hz), 130.2 (d, $J_{\text{CF}} = 8.4$ Hz), 132.2, 133.9, 141.4, 142.6 (d, $J_{\text{CF}} = 2.5$ Hz), 154.4, 159.5 (d, $^1J_{\text{CF}} = 246.8$ Hz), 163.4; MS, m/z : 652.2 $[\text{M} + \text{Na}]^+$.

tert-Butyl 4-((4-(4-(cyclohexyl)-1H-1,2,3-triazol-1-yl)phenyl)sulfonyl-4-(((tetrahydro-2H-pyran-2-yl)oxy)carbamoyl)piperidine-1-carboxylate (12i). Following the general procedure for the preparation of triazoles **12a–j**, from commercially available ethynylcyclohexane, and using 7:3 hexane–EtOAc as an eluent for chromatography, triazole **12i** (84 mg, 69%) was obtained as a beige solid, mp 101–102 °C. IR (KBr): 3321, 2933, 1695 cm^{-1} ; ^1H NMR (400 MHz, CDCl_3) δ 1.26–1.32 (m, 2H), 1.41–1.48 (m, 12H), 1.59–1.67 (m, 3H), 1.73–1.84 (m, 6H), 2.10–2.15 (m, 6H), 2.82–2.87 (m, 3H), 3.68–3.71 (m, 1H), 3.97–4.03 (m, 1H), 4.16 (br s, 2H), 5.01 (s, 1H), 7.77 (s, 1H), 7.96 (d, $J = 8.9$ Hz, 2H), 7.99 (d, $J = 8.9$ Hz, 2H), 9.47 (s, 1H); ^{13}C NMR (100 MHz, CDCl_3) δ 18.3, 25.0, 26.1, 26.1, 27.9, 28.1, 28.5, 32.9, 35.3, 40.7 (br), 62.5, 71.2, 80.3, 102.1, 117.4, 120.2, 132.1, 133.3, 141.8, 154.5, 155.3, 163.5; MS, m/z : 640.2 $[\text{M} + \text{Na}]^+$.

tert-Butyl 4-((4-(4-([1,1'-biphenyl]-3-yl)-1H-1,2,3-triazol-1-yl)phenyl)sulfonyl-4-(((tetrahydro-2H-pyran-2-yl)oxy)carbamoyl)-

piperidine-1-carboxylate (12j). Following the general procedure for the preparation of triazoles **12a–j**, from alkyne **14**, and using 6 : 4 hexane–EtOAc as an eluent for chromatography, triazole **12j** (78 mg, 59%) was obtained as a white solid, mp 136–137 °C. IR (KBr): 3269, 2924, 1695 cm⁻¹; ¹H NMR (400 MHz, CDCl₃) δ 1.45 (s, 9H), 1.60–1.70 (m, 3H), 1.80–1.87 (m, 3H), 2.14–2.21 (m, 4H), 2.87 (br s, 2H), 3.70–3.72 (m, 1H), 4.00–4.05 (m, 1H), 4.18 (br s, 2H), 5.03 (s, 1H), 7.38 (t, *J* = 7.4 Hz, 1H), 7.46 (t, *J* = 7.4 Hz, 2H), 7.53 (t, *J* = 7.7 Hz, 1H), 7.61 (d, *J* = 7.7 Hz, 1H), 7.66 (d, *J* = 7.4 Hz, 2H), 7.86 (d, *J* = 7.7 Hz, 1H), 8.04 (s, 4H), 8.14 (s, 1H), 8.35 (s, 1H), 9.50 (s, 1H); ¹³C NMR (100 MHz, CDCl₃) δ 18.3, 25.0, 27.9, 28.1, 28.5, 40.8 (br), 62.6, 71.2, 80.4, 102.1, 117.5, 120.4, 124.8, 124.9, 127.3, 127.8, 129.0, 129.6, 130.1, 132.2, 133.8, 140.7, 141.4, 142.2, 149.2, 154.5, 163.5; MS, *m/z*: 685.8 [M – H]⁻.

4-(4-(4-(Biphenyl-4-yl)-1H-1,2,3-triazol-1-yl)phenylsulfonyl)-N-hydroxypiperidine-4-carboxamide hydrochloride (13a). Following the general procedure for hydrochloride salts preparation, from **12a** (75 mg, 0.11 mmol), triazole **13a** (56 mg, 94%) was obtained as a beige solid, mp 247–248 °C (dec.). IR (KBr): 3358, 2947, 1660 cm⁻¹; ¹H NMR (300 MHz, DMSO-*d*₆) δ 2.17–2.25 (m, 2H), 2.54 (br s, 2H), 2.62–2.65 (m, 2H), 3.39–3.43 (m, 2H), 7.40 (t, *J* = 7.2 Hz, 1H), 7.50 (t, *J* = 7.2 Hz, 2H), 7.76 (d, *J* = 7.2 Hz, 2H), 7.85 (d, *J* = 8.2 Hz, 2H), 8.03 (d, *J* = 8.6 Hz, 2H), 8.07 (d, *J* = 8.2 Hz, 2H), 8.30 (d, *J* = 8.6 Hz, 2H), 8.87 (br s, 1H), 9.25 (br s, 1H), 9.65 (s, 1H), 11.27 (br s, 1H); ¹³C NMR (75.4 MHz, DMSO-*d*₆) δ 23.9, 40.3, 68.2, 119.9, 120.0, 125.9, 126.5, 127.3, 127.7, 128.8, 129.0, 132.3, 133.3, 139.4, 140.1, 140.7, 147.5, 159.4; MS, *m/z*: 504.1 [M + H]⁺; Anal. calcd for C₂₆H₂₆ClN₅O₄S + 1.2H₂O: C, 55.60; H, 5.10; N, 12.47; S, 5.71. Found: C, 55.69; H, 5.12; N, 12.00; S, 5.40.

N-Hydroxy-4-(4-(4-(4-pentylphenyl)-1H-1,2,3-triazol-1-yl)phenylsulfonyl)piperidine-4-carboxamide hydrochloride (13b). Following the general procedure for hydrochloride salts preparation, from **12b** (50 mg, 0.08 mmol), triazole **13b** (33 mg, 84%) was obtained as a pale yellow solid, mp 226–227 °C (dec.). IR (KBr): 3186, 2940, 2850, 1656 cm⁻¹; ¹H NMR (300 MHz, DMSO-*d*₆) δ 0.87 (t, *J* = 6.6 Hz, 3H), 1.30–1.31 (m, 4H), 1.58–1.63 (m, 2H), 2.18–2.26 (m, 2H), 2.54 (br s, 2H), 2.60–2.64 (m, 4H), 3.38–3.42 (m, 2H), 7.34 (d, *J* = 8.1 Hz, 2H), 7.87 (d, *J* = 8.1 Hz, 2H), 8.00 (d, *J* = 8.7 Hz, 2H), 8.28 (d, *J* = 8.7 Hz, 2H), 8.98 (br s, 1H), 9.39 (s, 1H), 9.50 (s, 1H), 11.23 (br s, 1H); ¹³C NMR (75.4 MHz, DMSO-*d*₆) δ 13.9, 21.9, 24.0, 30.5, 30.8, 34.9, 68.3, 119.4, 119.9, 125.4, 127.2, 128.9, 132.3, 133.3, 140.7, 142.9, 147.9, 159.5; MS, *m/z*: 498.2 [M + H]⁺; Anal. calcd for C₂₅H₃₂ClN₅O₄S + H₂O: C, 54.39; H, 6.21; N, 12.69; S, 5.81. Found: C, 54.56; H, 5.94; N, 12.66; S, 6.00.

4-((4-(4-(4-Methoxyphenyl)-1H-1,2,3-triazol-1-yl)phenyl)sulfonyl)-N-hydroxy-piperidine-4-carboxamide hydrochloride (13c). Following the general procedure for hydrochloride salts preparation, from **12c** (50 mg, 0.08 mmol), triazole **13c** (30 mg, 77%) was obtained as a pale yellow solid, mp 208–209 °C (dec.). IR (KBr): 3343, 3143, 2997, 2826, 1664 cm⁻¹; ¹H NMR (300 MHz, DMSO-*d*₆) δ 2.16–2.24 (m, 2H), 2.53 (br s, 2H), 2.64 (br s, 2H), 3.43 (br s, 2H), 3.82 (s, 3H), 7.10 (d, *J* = 8.8 Hz, 2H), 7.90 (d, *J* = 8.8 Hz, 2H), 8.01 (d, *J* = 8.8 Hz, 2H), 8.27 (d, *J* = 8.8 Hz, 2H),

8.81 (br s, 1H), 9.18 (br s, 1H), 9.42 (s, 1H), 9.45 (s, 1H), 11.26 (br s, 1H); ¹³C NMR (75.4 MHz, DMSO-*d*₆) δ 24.0, 55.3, 68.3, 114.5, 118.8, 119.9, 122.3, 126.9, 132.3, 133.2, 140.8, 147.8, 159.4, 159.5; MS, *m/z*: 458.0 [M + H]⁺; Anal. calcd for C₂₁H₂₄ClN₅O₅S + H₂O: C, 49.27; H, 5.12; N, 13.68; S, 6.26. Found: C, 48.48; H, 4.97; N, 13.10; S, 5.81.

N-Hydroxy-4-((4-(4-(4-phenoxyphenyl)-1H-1,2,3-triazol-1-yl)-phenyl)sulfonyl)piperidine-4-carboxamide hydrochloride (13d). Following the general procedure for hydrochloride salts preparation, from **12d** (62 mg, 0.09 mmol), triazole **13d** (49 mg, 98%) was obtained as a white solid, mp 231–233 °C (dec.). IR (KBr): 3196, 2969, 1667 cm⁻¹; ¹H NMR (300 MHz, DMSO-*d*₆) δ 2.12–2.21 (m, 2H), 2.62–2.73 (m, 2H), 3.43 (“br s”, 2H), 7.09 (d, *J* = 7.7 Hz, 2H), 7.15–7.22 (m, 3H), 7.44 (t, *J* = 7.7 Hz, 2H), 7.96–8.03 (m, 4H), 8.27 (d, *J* = 8.8 Hz, 2H), 8.66 (br s, 1H), 8.97 (br s, 1H), 9.41 (s, 1H), 9.52 (s, 1H), 11.26 (s, 1H); ¹³C NMR (75.4 MHz, DMSO-*d*₆) δ 24.0, 40.4, 68.3, 118.9, 119.0, 119.5, 120.0, 123.8, 125.0, 127.3, 130.2, 132.3, 133.3, 140.7, 147.4, 156.3, 157.0; MS, *m/z*: 520.1 [M + H]⁺; Anal. calcd for C₂₆H₂₆ClN₅O₅S + H₂O: C, 54.40; H, 4.92; N, 12.20; S, 5.59. Found: C, 54.14; H, 4.83; N, 11.71; S, 5.21.

4-((4-(4-(4-(Dimethylamino)phenyl)-1H-1,2,3-triazol-1-yl)-phenyl)sulfonyl)-N-hydroxypiperidine-4-carboxamide dihydrochloride (13e). Following the general procedure for hydrochloride salts preparation, from **12e** (50 mg, 0.08 mmol), triazole **13e** (28 mg, 69%) was obtained as a white solid, mp 216–217 °C (dec.). IR (KBr): 3388, 2925, 1664 cm⁻¹; ¹H NMR (300 MHz, D₂O) δ 2.37–2.56 (m, 4H), 2.92–3.00 (m, 2H), 3.28 (s, 6H), 3.57–3.62 (m, 2H), 7.63 (d, *J* = 8.8 Hz, 2H), 7.96 (d, *J* = 8.8 Hz, 2H), 8.00 (d, *J* = 8.9 Hz, 2H), 8.09 (d, *J* = 8.9 Hz, 2H), 8.93 (s, 1H); ¹³C NMR (75.4 MHz, D₂O) δ 24.3, 40.7, 46.3, 68.6, 120.7, 121.0, 121.2, 127.6, 130.7, 132.1, 141.1, 142.2, 146.8, 161.8; MS, *m/z*: 471.3 [M + H]⁺; Anal. calcd for C₂₂H₂₈Cl₂N₆O₄S + 3H₂O: C, 44.22; H, 5.74; N, 14.06; S, 5.37. Found: C, 44.18; H, 5.55; N, 13.17; S, 5.26.

4-((4-(4-(4-Fluorophenyl)-1H-1,2,3-triazol-1-yl)phenyl)sulfonyl)-N-hydroxypiperidine-4-carboxamide hydrochloride (13f). Following the general procedure for hydrochloride salts preparation, from **12f** (65 mg, 0.10 mmol), triazole **13f** (47 mg, 98%) was obtained as a white solid, mp 219–220 °C (dec.). IR (KBr): 3197–2743, 1660 cm⁻¹; ¹H NMR (400 MHz, DMSO-*d*₆) δ 2.13–2.18 (m, 2H), 2.61–2.67 (m, 2H), 3.38–3.41 (m, 2H), 7.39 (t, *J* = 8.8 Hz, 2H), 7.99–8.03 (m, 4H), 8.26 (d, *J* = 8.6 Hz, 2H), 8.61 (br s, 1H), 9.37 (br s, 1H), 9.53 (s, 1H), 11.19 (br s, 1H); ¹³C NMR (100 MHz, DMSO-*d*₆) δ 24.2, 40.7, 116.1 (d, ²*J*_{CF} = 21.6 Hz), 119.9, 120.1, 126.4 (d, ⁴*J*_{CF} = 3.0 Hz), 127.6 (d, ³*J*_{CF} = 8.2 Hz), 132.3, 132.4, 133.5, 140.7, 147.0; HPLC-MS, purity >95%, *m/z*: 446 [M + H]⁺.

4-(4-(4-(3-Fluorophenyl)-1H-1,2,3-triazol-1-yl)phenyl)sulfonyl)-N-hydroxypiperidine-4-carboxamide hydrochloride (13g). Following the general procedure for hydrochloride salts preparation, from **12g** (70 mg, 0.11 mmol), triazole **13g** (45 mg, 84%) was obtained as a white solid, mp 215–216 °C (dec.). IR (KBr): 2981, 1657, 1590 cm⁻¹; ¹H NMR (300 MHz, DMSO-*d*₆) δ 2.17–2.25 (m, 2H), 2.53 (br s, 2H), 2.61–2.64 (m, 2H), 3.42 (br s, 2H), 7.26 (td, *J* = 8.8, 2.5 Hz, 1H), 7.58 (m, 1H), 7.78 (d, *J* =

9.3 Hz, 1H), 7.83 (d, $J = 7.9$ Hz, 1H), 8.02 (d, $J = 8.8$ Hz, 2H), 8.27 (d, $J = 8.8$ Hz, 2H), 8.98 (br s, 1H), 9.43 ("br s", 2H), 9.67 (s, 1H), 11.27 (s, 1H); ^{13}C NMR (75.4 MHz, DMSO- d_6) δ 24.0, 68.3, 112.1 (d, $^2J_{\text{CF}} = 22.8$ Hz), 115.4 (d, $^2J_{\text{CF}} = 21.4$ Hz), 120.1, 120.8, 121.5 (d, $^4J_{\text{CF}} = 2.8$ Hz), 131.4 (d, $^3J_{\text{CF}} = 8.8$ Hz), 132.2 (d, $^3J_{\text{CF}} = 8.5$ Hz), 132.4, 133.5, 140.6, 146.8, 159.5, 162.6 (d, $^1J_{\text{CF}} = 233.7$ Hz); HPLC-MS, purity >93%, m/z : 446.2 $[\text{M} + \text{H}]^+$.

4-((4-(2-Fluorophenyl)-1H-1,2,3-triazol-1-yl)phenyl)sulfonyl)-N-hydroxypiperidine-4-carboxamide hydrochloride (13h). Following the general procedure for hydrochloride salts preparation, from **12h** (80 mg, 0.13 mmol), triazole **13h** (55 mg, 90%) was obtained as a white solid, mp 238–239 °C (dec.). IR (KBr): 3176–2992, 1660 cm^{-1} ; ^1H NMR (400 MHz, DMSO- d_6) δ 2.18–2.24 (m, 2H), 2.53 (br s, 2H), 2.61–2.67 (m, 2H), 3.39–3.42 (m, 2H), 7.37–7.44 (m, 2H), 7.47–7.52 (m, 1H), 7.99 (d, $J = 8.7$ Hz, 2H), 8.21 (t, $J = 6.6$ Hz, 1H), 8.36 (d, $J = 8.7$ Hz, 2H), 8.90 (br s, 1H), 9.30 (d, $J = 3.4$ Hz, 1H), 9.38 (s, 1H), 11.24 (br s, 1H); ^{13}C NMR (100 MHz, DMSO- d_6) δ 24.0, 40.4, 68.3, 116.2 (d, $J_{\text{CF}} = 20.8$ Hz), 117.6 (d, $J_{\text{CF}} = 13.1$ Hz), 120.5, 122.0 (d, $J_{\text{CF}} = 10.5$ Hz), 125.1 (d, $J_{\text{CF}} = 3.4$ Hz), 127.8 (d, $J_{\text{CF}} = 3.1$ Hz), 130.5 (d, $J_{\text{CF}} = 8.7$ Hz), 132.1, 133.5, 140.6, 141.5 (d, $J_{\text{CF}} = 2.3$ Hz), 158.6 (d, $^1J_{\text{CF}} = 247.2$ Hz), 159.5; HPLC-MS, purity >95%, m/z : 446 $[\text{M} + \text{H}]^+$.

4-((4-(4-Cyclohexyl-1H-1,2,3-triazol-1-yl)phenyl)sulfonyl)-N-hydroxypiperidine-4-carboxamide hydrochloride (13i). Following the general procedure for hydrochloride salts preparation, from **12i** (84 mg, 0.14 mmol), triazole **13i** (63 mg, 96%) was obtained as a beige solid, mp 216–217 °C (dec.). IR (KBr): 3194–2906, 1660 cm^{-1} ; ^1H NMR (400 MHz, DMSO- d_6) δ 1.21–1.30 (m, 1H), 1.36–1.51 (m, 4H), 1.69–1.73 (m, 1H), 1.77–1.80 (m, 2H), 2.03–2.05 (m, 2H), 2.12–2.19 (m, 2H), 2.46 (1H, "under DMSO"), 2.63 (t, $J = 13.7$, 2H), 2.76–2.80 (m, 1H), 3.38–3.41 (m, 2H), 7.94 (d, $J = 8.8$ Hz, 2H), 8.20 (d, $J = 8.8$ Hz, 2H), 8.79 ("s", 2H), 9.36 (br s, 1H), 11.17 (br s, 1H); ^{13}C NMR (100 MHz, DMSO- d_6) δ 24.0, 25.4, 25.6, 32.3, 34.5, 40.4, 68.2, 119.3, 119.8, 132.2, 132.9, 140.9, 153.9, 159.5; HPLC-MS, purity >95%, m/z : 434 $[\text{M} + \text{H}]^+$.

4-((4-([1,1'-Biphenyl]-3-yl)-1H-1,2,3-triazol-1-yl)phenyl)sulfonyl)-N-hydroxypiperidine-4-carboxamide hydrochloride (13j). From **12j** (70 mg, 0.10 mmol), triazole **13j** (54 mg, 100%) was obtained as a beige solid, mp 228–229 °C (dec.). IR (KBr): 3199–2983, 1655 cm^{-1} ; ^1H NMR (400 MHz, DMSO- d_6) δ 2.18–2.24 (m, 2H), 2.53 (br s, 2H), 2.60–2.69 (m, 2H), 7.43 (t, $J = 7.3$ Hz, 1H), 7.53 (t, $J = 7.7$ Hz, 2H), 7.63 (t, $J = 7.7$ Hz, 1H), 7.72 (d, $J = 7.7$ Hz, 1H), 7.77 (d, $J = 7.4$ Hz, 2H), 7.99–8.04 (m, 3H), 8.25–8.30 (m, 3H), 8.86 (br s, 1H), 9.25 (br s, 1H), 9.68 (s, 1H), 11.23 (s, 1H); ^{13}C NMR (100 MHz, DMSO- d_6) δ 24.0, 40.4, 68.3, 120.0, 120.2, 123.8, 124.3, 126.8, 126.9, 127.8, 129.0, 129.8, 130.4, 132.3, 133.4, 139.7, 140.7, 141.0, 147.8, 159.4; HPLC-MS, purity >94%, m/z : 504 $[\text{M} + \text{H}]^+$.

3-Ethynyl-1,1'-biphenyl (14). To a solution of [1,1'-biphenyl]-3-carbaldehyde (200 mg, 1.10 mmol, 1.00 eq.) in anhydrous MeOH (4 mL) under argon were added dry K_2CO_3 (456 mg, 3.30 mmol, 3.00 eq.) and freshly prepared BOR (421 mg, 2.20 mmol, 2.00 eq.). The resulting mixture was stirred at rt for 1 h. The reaction mixture was concentrated. The residue was

solved in EtOAc, and the solution was washed twice with water and brine, dried (anhydrous MgSO_4), filtered and evaporated to give 166 mg of a yellow oil. The crude product was purified by chromatography on silica gel (hexane as an eluent) to afford **14** (140 mg, 71%) as a colourless oil. IR (KBr): 3305, 2102 cm^{-1} ; ^1H NMR (300 MHz, CDCl_3) δ 3.13 (s, 1H), 7.36–7.52 (m, 5H), 7.58–7.62 (m, 3H), 7.76–7.77 (m, 1H); ^{13}C NMR (75.4 MHz, CDCl_3) δ 77.4, 83.8, 122.7, 127.2, 127.8, 128.9, 129.0, 131.0, 140.3, 141.5.

NMR experiments

All spectra were recorded at 300 K using a Bruker Avance III 500 MHz spectrometer equipped with a 5 mm broadband TBI probe. A typical NMR sample contained a concentration of 5 μM of MMP-2 (expression and purification details of this MMP-2 construct will be published elsewhere) and 100 μM of ligand (from a 50 mM stock in DMSO- d_6), in an approximate protein : ligand ratio of 1 : 20, optimal for the water-LOGSY experiments. To 450 μL of the sample (buffer: 10 mM deuterated-Tris/HCl, pH 7.4, with 50 mM NaCl, 0.02% NaN_3 , 100 μM CaCl_2 and 100 μM ZnCl_2) 25 μL of D_2O were added for locking purposes, and 25 μL of DMSO- d_6 to increase the solubility of the compounds. BiPS (2R-[(4-biphenylsulfonyl)amino]-N-hydroxy-3-phenylpropinamide; VWR, Barcelona, Spain) was used for the competition experiments from a 50 mM stock in DMSO- d_6 . For each sample, 1D ^1H and waterLOGSY (direct interaction and competition) experiments were recorded. 8 K points were used for a sweep width of 9600 Hz and a total of 512 scans were accumulated for the waterLOGSY experiment. In these experiments, the large bulk water magnetization is partially transferred *via* the protein–ligand complex to the free ligand in a selective manner. A non-interacting compound results in negative resonances, whereas protein–ligand interactions are characterized by positive signals or by a reduction in the negative signals obtained in the absence of the protein.

Solubility

The solubility in water (MQ water was used) at 25 °C was determined by UV spectroscopy. The absorbance of four solutions at different solute concentrations was measured to construct a calibration curve. The absorbance of a saturated solution was measured and plotted to estimate the solubility, using the Beer–Lambert law. Each sample was centrifuged and the supernatant was taken for absorbance measurement. Each experiment was repeated three times, and the mean values were calculated.

Biology

Matrix metalloproteinase activity inhibition. MMPs activity measurements were performed using an *MMP Inhibitor Profiling Kit* purchased from Enzo Life Science International, Inc., following the manufacturer's protocol with slight modifications. Proteolytic activity was measured using a thiopeptide substrate (Ac-PLG-[2-mercapto-4-methylpentanoyl]-LG- OC_2H_5) where the MMP cleavage site peptide bond has been replaced by a thioester bond.^{42,43} Hydrolysis of this bond by MMP

produces a sulfhydryl group that reacts with DTNB to form 2-nitro-5-thiobenzoic acid, which was detected by its absorbance at 414 nm (microplate photometer Thermo Scientific Multiscan FC). Enzyme reactions were carried out at 37 °C in a 100 µL final volume of solutions, where the catalytic domains of the corresponding MMP were incubated in triplicate with at least seven concentrations of inhibitors. The assay buffer contained the following components: 50 mM HEPES, 10 mM CaCl₂, 0.05% Brij-35 and 1 mM DTNB at pH 7.5. After addition of the substrate, the increase of absorbance was recorded in 1 min time intervals for 30 min. Data were plotted as OD *versus* time for each sample in order to obtain the reaction velocity (*V*) in OD per min. The percentage of residual activity for each compound was calculated using the following formula: % of remaining activity = (*V* in the presence of inhibitor/*V* control) × 100. An inhibitor, NNGH, was included as a prototypic control inhibitor.⁴⁴ The concentration of compound that provides 50% inhibition of enzymatic activity (IC₅₀) was determined by semi-logarithmic dose–response plots (*Graph Pad Prism 5.0 for Windows*, Graph Pad Software Inc., San Diego, California, USA, 2007).

HDAC activity inhibition. The inhibitory potential of compounds towards histone deacetylases has been established with an *HDAC Colorimetric/Drug Discovery Kit* (Enzo Life Science International, Inc.). The colorimetric substrate, which contains an acetylated lysine side chain, is incubated (37 °C) with a HeLa nuclear extract (rich in HDAC activity, especially HDAC1 and HDAC2) and a range of concentrations of the inhibitor. The substrate is sensitized by deacetylation and, in a second step, reacts with the developer causing an increase in the absorption at 405 nm. Trichostatin A was used as the positive control.

Cell culture. HT1080 (human fibrosarcoma) cells were maintained as monolayer cultures in MEM (Gibco) medium, supplemented with 10% heat-inactivated FBS (Lonza) and penicillin–streptomycin (100 IU mL^{−1}–100 µg mL^{−1}). The growth inhibitory effect of compounds was evaluated by using the MTT assay. Briefly, cells were seeded into 96-well plates at 3000 cells per well and allowed to adhere 24 h prior to addition of the compounds. The cells were then washed twice with PBS, and treated with various concentrations of compounds (diluted in serum-free medium) for 24 h. Four hours before the end of incubation, 20 µL of MTT solution (5 mg mL^{−1}) was added to each well. Formazan crystals in the wells were solubilized in 200 µL of DMSO (Panreac). The absorbance was measured at 570 nm wavelength using a spectrophotometer (Biotec). The assay was repeated in three independent experiment replications. The viability was calculated by considering controls containing the solvent control (0.1% DMSO) to be 100% viable.

Invasion assay. To evaluate the anti-invasiveness of compounds **1a–i** and **13a–h**, a fluorimetric QCM ECMatrix Cell Invasion Assay (Millipore) was used by following the protocol of the manufacturer with minor modifications. The assay was performed in a 96-well invasion plate based on the Boyden Chamber principle. The HT1080 cells were starved overnight

in FBS-free medium followed by harvesting and placing 0.1×10^6 cells resuspended in FBS-free medium (containing 0.5% BSA) in each well. The lower portion of the chamber contained a medium with 10% FBS as a chemoattractant. The compounds were added to the cell suspension in triplicates. Cells were incubated in the absence (solvent control 0.1% DMSO) and presence of the compounds for 22 h. Invasive cells able to invade through a layer of basement membrane matrix solution and crossing the pores of the polycarbonate membrane were dissociated from the membrane and detected with CyQuantGR dye. The fluorescence was read with a fluorescence plate reader at 480 nm/520 nm (Synergy Mx, Biotec).

Transport experiments across the Caco-2 monolayer. Caco-2 cells were grown in DMEM (Gibco) medium supplemented with 10% FBS (Lonza), 1% NEAA, 50 U mL^{−1} penicillin and 50 µg mL^{−1} streptomycin (Gibco). For transport experiments 0.3×10^6 cells per insert were seeded on 12 mm Transwell inserts with a 0.4 µm pore polyethylene terephthalate (PET) membrane. Cells were allowed to differentiate for 21 days, with medium being replaced every second day. The cell monolayer integrity was monitored by measuring the transepithelial electrical resistance (TEER) using a Mini-ERS Volt/ohmmeter (Millipore Corp., Bedford, MA). TEER values higher than 250 Ω cm² were chosen for transport studies.

Transport experiment. Prior to experiments, the cells were washed twice with FBS-free DMEM medium. **13e** was dissolved in FBS-free medium to final concentrations of 10 and 5 µM. Absorptive transport experiments were performed from apical to basolateral (A to B) and secretive from basolateral to apical (B to A) sides of the cell monolayer. At 2 time points (1 h and 2 h) aliquots were collected from the receiver compartment and the amounts removed were replaced with FBS-free DMEM. The concentration of the samples was analyzed by LC/MS-QQQ.

LC/MS-QQQ quantitative analysis. The Caco-2 samples as well as standards (different concentrations of **13e**, ranging from 0.1 µM to 15 µM diluted in the assay medium) were pre-treated before analysis to precipitate proteins, by adding three volumes of cool acetonitrile to one volume of the sample and centrifuged for 15 min at 12 000 r.p.m. The supernatant containing the compound was immediately withdrawn. The obtained samples were analyzed by LC/MS-QQQ using an Agilent 1290 chromatograph and an Agilent 6460 mass spectrometer equipped with an ESI source type “jet stream” and a triple quadrupole analyzer (QQQ). Firstly, a gradient chromatographic method (RP-HPLC) was developed using an analytical column Ascentis Express C18 (100 × 2, 1 mm, 2.7 µm) from Supelco. The mobile phases consisted of A: MilliQ water, 0.1% formic acid, and B: methanol, 0.1% formic acid. A gradient of 5% of B, increasing to 95% in 20 min, 2 min at 95% and returning to 5% at 23 min, followed by 5 min of re-equilibration of the column was used. The injection volume was 10 µL and the flow rate was 0.3 mL min^{−1}.

A flow injection analysis of 1 µM solution of **13e** was carried out for optimization of the mass spectrometer conditions which were finally established to be: polarity positive,

nebulizer gas and drying-nitrogen, gas flow 8 L min⁻¹, nebulizer gas pressure 45 psi, drying gas temperature 300 °C. In order to get maximum selectivity and sensitivity the MRM (multiple reaction monitoring) procedure was employed. MRM transitions achieved for **13e** were: 471→283 (quantification) and 471→235.6 (qualification) with a V fragmentor (135 V), dwell time (200 ms) and collision energies (20 eV) in both cases.

Apparent permeability coefficient (P_{app})

The apparent permeability coefficient (P_{app}) in cm s⁻¹ was determined from the following formula: $P_{app} = V_d C / dT A C_0$, where V = volume of the sample (mL), dC = concentration variations, dT = time variations, dQ = quantity variations, C_0 = the initial concentration in the donor compartment and A = exposed surface in cm².^{45,46} The efflux ratio was calculated from the equation: $P_{app,ba} / P_{app,ab}$.

Computational methods

Preparation of the protein structures. For MMP-2, we chose the structure 10 of 1HOV PDB,³⁷ in which SC-74020 is complexed to the MMP-2 catalytic domain that does not contain the three fibronectin-like inserts. The positions of each residue and metal (Zn²⁺ and Ca²⁺ ions) were kept for docking.

For MMP-9, we selected the 2OW1 crystal structure (chain A) of the isolated catalytic domain,²¹ which presents a Gln402Glu mutation at the active site (Glu₁₂₁ in the 1HOV numbering) and a trifluoromethyl hydroxamate inhibitor bound to the catalytic site. The catalytic Gln₄₀₂ was computationally mutated back to Glu residue and Zn²⁺ and Ca²⁺ ions were kept for docking experiments.

Docking setting. Flexible docking calculations were carried out with the Glide program,^{47–49} using default parameters and requiring a maximum of ten output poses. We selected the XP (Extra-Precision) method allowing a more extensive sampling method, as well as a more exigent scoring function.⁵⁰ We removed all water molecules and counterions (chlorine) in the 1HOV and 2OW1 experimental structures. The proteins were prepared using the protein preparation wizard⁵¹ provided in the Schrödinger suite and the grids were constructed with the grid receptor generation module included in Glide software. During the docking calculations, all the protein residues were fixed and only the inhibitor atoms were allowed to move. The catalytic zinc ion and Glu₁₂₁ side chain were assigned a +2 and -1 charge, respectively, whereas the ligands were built with a neutral hydroxamic moiety and a positively charged piperidine group. The ligand was prepared using LigPrep⁵² application also provided in the Schrödinger suite.

Molecular dynamics simulation. The initial structure of the MMP-2:13e complex was obtained from the superimposition of the docking pose of **13e** in 1HOV and 1CK7 catalytic centers (1CK7, which corresponds to the Ala404Glu mutant of the full-length pro-MMP-2 enzyme). The propeptide (Pro₃₁-Asn₁₀₉, 1CK7 numbering) and the C-terminal hemopexin-domain (Leu₄₆₁-Cys₆₆₀) were deleted from the initial crystal structure, and the three fibronectin-type domains (Glu₂₁₇-Gln₃₉₃) that

characterize gelatinases were replaced by a short peptide segment (Lys-Gly-Val) as in the 1QIB crystal structure of the catalytic domain. Two zinc and two calcium ions were kept in the positions observed in the initial structure, thus resulting in a global charge for the catalytic domain of -3. 1CK7 was preferred for MD simulations, as the 1HOV structure appeared to be unstable after several attempts. Direct docking of **13e** in 1CK7 did not give satisfactory poses, due to the thin opening of the S1' pocket in this MMP-2 structure and manual superimposition was thus used.

Binding of **13e** hydroxamate group (deprotonated form) to the catalytic zinc ion and the protonation state of Glu₁₂₁ (neutral) in MMP-2 were modeled as reported in a previous work³⁸ and QM/MM calculations that will be published elsewhere. The system was subsequently surrounded by a periodic box of TIP3P water molecules that extended 15 Å from the protein atoms, and Na⁺ counterions were placed to neutralize the systems. This resulted in a total of ~2550 protein atoms being solvated by ~17 000 water molecules.

The catalytic and the structural zinc ions as well as the two Ca(II) ions were kept in all the MD simulations. For the Ca(II) ions, we employed the non-bonded representation proposed by Aqvist.⁵³ For the structural zinc ion we used a set of MM parameters that have been developed in the context of the parm03 force field and tested by us in a previous work.⁵⁴ The interaction between the catalytic zinc ion and the inhibitor was also modeled using a bonded representation in which the metal ion is linked to the His₄₀₃-Ne, His₄₀₈-Ne, His₄₁₃-Ne atoms of the protein (1CK7 numbering) and to the O1 atom of the **13e** hydroxamate group by explicit MM bonds. In contrast, the coordination of **13e** to the Zn₁ ion through the carbonyl O2 atom of the hydroxamate group is represented by non-bonded parameters. We computed the atomic partial charges of **13e**, His₄₀₃, Glu₄₀₄, His₄₀₈, His₄₁₃ (1CK7 numbering) and the catalytic zinc ion using the RESP methodology^{55,56} at the B3LYP/cc-pVTZ level of theory and using the IEFPCM continuum solvent model ($\epsilon = 4$). During the RESP fitting procedure we assigned a zero value to the atomic charges of the H-link atoms of the protein residues and to the three H atoms of the methyl group of the ligand. We also imposed a global charge of +0.048548e for the protonated Glu₄₀₄ side chain (parm03 value).

Force constants for the bond (Zn₁-X) and angle (Zn₁-X-Y and X-Zn₁-Y) MM terms were assigned a similar value (120.0). All the torsions associated with the zinc-ligand interactions were set to zero. The van der Waals parameters for the Zn₁ ion were taken from our previous parameterization of the native MMP-2.⁵⁴ The rest of the atoms in the imidazole rings and the glutamic acid side chain were assigned the corresponding standard AMBER atom types. For **13e**, we selected appropriate atom types from the AMBER *gaff* force field.⁵⁷

MD simulation was carried out using the SANDER and PMEMD programs included in the Amber 11 suite of programs.⁵⁸ The solvent molecules and counterions were initially relaxed by means of energy minimizations and 50 ps of MD. Then the full systems were minimized to remove bad contacts

in the initial geometry and heated gradually to 300 K during 60 ps of MD. The SHAKE algorithm was employed to constrain all R–H bonds, and periodic boundary conditions were applied to simulate a continuous system. A non-bonded cutoff of 10.0 Å was used and the Particle-Mesh-Ewald (PME) method was employed to include the contributions of long-range interactions. The pressure (1 atm) and the temperature (300 K) of the system were controlled during the MD simulations by Berendsen's method. A 100 ns trajectory was computed with a time step of 2 fs and using the GPU-accelerated version of the PMEMD code included in Amber 11. The recommended SPDP precision model, which provides an optimum trade-off between accuracy and performance, was employed in the GPU-accelerated simulations. Coordinates were saved for analysis every 2 ps.

Structural analyses of the MD trajectories. Structural analyses were carried out using the PTRAJ module of Amber 11 by applying classical geometrical criteria for monitoring the interactions listed in the Discussion section.

Abbreviations

A	Apical
B	Basolateral
BOR	Bestmann–Ohira reagent
<i>c log D</i>	Calculated distribution coefficient
CuAAC	Copper catalysed azide–alkyne cycloadditions
DMEM	Dulbecco's modified Eagle's medium
DTNB	5,5'-Dithiobis-(2-nitrobenzoic acid)
ECM	Extracellular matrix
EDCI	1-Ethyl-3-(3-dimethylaminopropyl)-carbodiimide
FBS	Fetal bovine serum
GPU	Ground power unit
HEPES	4-(2-Hydroxyethyl)-1-piperazineethanesulfonic acid
HOBt	Hydroxybenzotriazole
MCPBA&TAB1;	Meta-chloroperoxybenzoic acid
MM	Molecular mechanics
MMPI	MMP inhibitor
MTT	3-(4,5-Dimethylthiazol-2-yl)-2,5-diphenyltetrazolium bromide
NMM	<i>N</i> -Methylmorpholine
NNGH	<i>N</i> -Isobutyl- <i>N</i> -(4-methoxyphenylsulfonyl)glycyl hydroxamic acid
Papp	Apparent permeability coefficients
PME	Particle-Mesh-Ewald
QM	Quantum mechanical
RMSD	Root mean square deviation
SD	Standard deviation
STD	Saturation transfer difference
TEER	Transepithelial electrical resistance
waterLOGSY	Water ligand observed <i>via</i> gradient spectroscopy
ZBG	Zinc binding group

Acknowledgements

This work was supported by the Spanish Ministry of Science and Innovation (SAF2008-00945, CTQ2011-24741, CTQ2007-63226, and SAF2011-28350). R. J. C. thanks the Spanish Ministry of Science for a Ramón y Cajal contract. Grants to B. F. and K. F. from Fundación Universitaria San Pablo CEU are also acknowledged. B. F. also thanks CEU-Banco Santander for the “becas de movilidad para jóvenes investigadores y profesores universitarios”. We thank Dr Sonia de Pascual-Teresa and her team from the ICTAN, CSIC, for providing the material necessary for solubility determination and cellular assays, as well as valuable suggestions and assistance in cell experiments. We thank Synthelia Organics SL for HPLC-MS experiments. Part of this work was awarded the “Premio Ramón Madroño”, given by the Sociedad Española de Química Terapéutica (SEQT), Spain in 2013.

Notes and references

- 1 M. D. Sternlicht and Z. Werb, *Annu. Rev. Cell Dev. Biol.*, 2001, **17**, 463–516.
- 2 Degradome <http://degradome.uniovi.es/> or MEROPS database <http://www.merops.sanger.ac.uk/>
- 3 C. M. Overall and O. Kleifeld, *Nat. Rev. Cancer*, 2006, **6**, 227–239.
- 4 P. Serra, M. Bruczko, J. Zapico, A. Puckowska, M. García, S. Martín-Santamaría, A. Ramos and B. de Pascual-Teresa, *Curr. Med. Chem.*, 2012, **19**, 1036–1064.
- 5 D. P. Becker, C. I. Villamil, T. E. Barta, L. J. Bedell, T. L. Boehm, G. A. DeCrescenzo, J. N. Freskos, D. P. Getman, S. Hockerman and R. Heintz, *J. Med. Chem.*, 2005, **48**, 6713–6730.
- 6 D. P. Becker, T. E. Barta, L. J. Bedell, T. L. Boehm, B. R. Bond, J. Carroll, C. P. Carron, G. A. DeCrescenzo, A. M. Easton and J. N. Freskos, *J. Med. Chem.*, 2010, **53**, 6653–6680.
- 7 S. A. Kolodziej, S. L. Hockerman, G. A. DeCrescenzo, J. J. McDonald, D. A. Mischke, G. E. Munie, T. R. Fletcher, N. Stehle, C. Swearingen and D. P. Becker, *Bioorg. Med. Chem. Lett.*, 2010, **20**, 3561–3564.
- 8 S. A. Kolodziej, S. L. Hockerman, T. L. Boehm, J. N. Carroll, G. A. DeCrescenzo, J. J. McDonald, D. A. Mischke, G. E. Munie, T. R. Fletcher, J. G. Rico, N. W. Stehle, C. Swearingen and D. P. Becker, *Bioorg. Med. Chem. Lett.*, 2010, **20**, 3557–3560.
- 9 K. Maskos, *Biochimie*, 2005, **87**, 249–263.
- 10 L. Devel, B. Czarny, F. Beau, D. Georgiadis, E. Stura and V. Dive, *Biochimie*, 2010, **92**, 1501–1508.
- 11 J. M. Zapico, P. Serra, J. Garcia-Sanmartin, K. Filipiak, R. J. Carbajo, A. K. Schott, A. Pineda-Lucena, A. Martinez, S. Martin-Santamaria, A. Ramos and B. de Pascual-Teresa, *Org. Biomol. Chem.*, 2011, **9**, 4587–4599.
- 12 I. Schechter and A. Berger, *Biochem. Biophys. Res. Commun.*, 1967, **27**, 157.

- 13 J. Pietruszka and A. Witt, *Synthesis*, 2006, 4266–4268.
- 14 P. Serra, Ph.D. dissertation, Universidad CEU San Pablo, Madrid (Spain), 2012.
- 15 T. S. McDermott, L. Bhagavatula, T. B. Borchardt, K. M. Engstrom, J. Gandarilla, B. J. Kotecki, A. W. Kruger, M. J. Rozema, A. Y. Sheikh and S. H. Wagaw, *Org. Process Res. Dev.*, 2009, **13**, 1145–1155.
- 16 C. Dalvit, P. Pevarello, M. Tatò, M. Veronesi, A. Vulpetti and M. Sundström, *J. Biomol. NMR*, 2000, **18**, 65–68.
- 17 B. Meyer and T. Peters, *Angew. Chem., Int. Ed.*, 2003, **42**, 864–890.
- 18 M. Gooyit, M. Lee, V. A. Schroeder, M. Ikejiri, M. A. Suckow, S. Mobashery and M. Chang, *J. Med. Chem.*, 2011, **54**, 6676–6690.
- 19 A. L. Hopkins, C. R. Groom and A. Alex, *Drug Discovery Today*, 2004, **9**, 430.
- 20 I. Kuntz, K. Chen, K. Sharp and P. Kollman, *Proc. Natl. Acad. Sci. U. S. A.*, 1999, **96**, 9997.
- 21 A. Tochowicz, K. Maskos, R. Huber, R. Oltenfreiter, V. Dive, A. Yiotakis, M. Zanda, W. Bode and P. Goettig, *J. Mol. Biol.*, 2007, **371**, 989–1006.
- 22 B. Lovejoy, A. R. Welch, S. Carr, C. Luong, C. Broka, R. T. Hendricks, J. A. Campbell, K. A. Walker, R. Martin, H. Van Wart and M. F. Browner, *Nat. Struct. Biol.*, 1999, **6**, 217–221.
- 23 S. Rowsell, P. Hawtin, C. A. Minshull, H. Jepson, S. Brockbank, D. G. Barratt, A. M. Slater, W. L. McPheat, D. Waterson and A. M. Henney, *J. Mol. Biol.*, 2002, **319**, 173–181.
- 24 W. K. Hagmann, *J. Med. Chem.*, 2008, **51**, 4359.
- 25 K. Müller, C. Faeh and F. Diederich, *Science*, 2007, **317**, 1881–1886.
- 26 J. A. Olsen, D. W. Banner, P. Seiler, U. Obst Sander, A. D'Arcy, M. Stihle, K. Müller and F. Diederich, *Angew. Chem., Int. Ed.*, 2003, **42**, 2507–2511.
- 27 J. Olsen, P. Seiler, B. Wagner, H. Fischer, T. Tschopp, U. Obst-Sander, D. W. Banner, M. Kansy, K. Müller and F. Diederich, *Org. Biomol. Chem.*, 2004, **2**, 1339–1352.
- 28 D. E. Kleiner and W. G. Stetler-Stevenson, *Cancer Chemother. Pharmacol.*, 1999, **43**, S42–S51.
- 29 A. R. Nelson, B. Fingleton, M. L. Rothenberg and L. M. Matrisian, *J. Clin. Oncol.*, 2000, **18**, 1135–1149.
- 30 P. Basset, A. Okada, M. P. Chenard, R. Kannan, I. Stoll, P. Anglard, J. P. Bellocq and M. C. Rio, *Matrix Biol.*, 1997, **15**, 535–541.
- 31 R. L. Wynn, *Gen. Dent.*, 1999, **47**, 19–22.
- 32 A. Vannini, C. Volpari, G. Filocamo, E. C. Casavola, M. Brunetti, D. Renzoni, P. Chakravarty, C. Paolini, R. De Francesco and P. Gallinari, *Proc. Natl. Acad. Sci. U. S. A.*, 2004, **101**, 15064.
- 33 A. Vannini, C. Volpari, P. Gallinari, P. Jones, M. Mattu, A. Carfi, R. De Francesco, C. Steinkühler and S. Di Marco, *EMBO Reports*, 2007, **8**, 879–884.
- 34 I. J. Hidalgo, T. Raub and R. Borchardt, *Gastroenterology*, 1989, **96**, 736.
- 35 V. Pade and S. Stavchansky, *J. Pharm. Sci.*, 1998, **87**, 1604–1607.
- 36 <http://www.drugbank.ca>
- 37 Y. Feng, J. J. Likos, L. Zhu, H. Woodward, G. Munie, J. J. McDonald, A. M. Stevens, C. P. Howard, G. A. De Crescenzo and D. Welsch, *Biochim. Biophys. Acta*, 2002, **1598**, 10–23.
- 38 B. Jason, J. S. Duca, J. J. Kaminski and V. S. Madison, *J. Am. Chem. Soc.*, 2002, **124**, 11004–11007.
- 39 P. C. Chen, R. E. Wharton, P. A. Patel and A. K. Oyelere, *Bioorg. Med. Chem.*, 2007, **15**, 7288–7300.
- 40 M. A. Matulenko, E. S. Paight, R. R. Frey, A. Gomtsyan, S. DiDomenico Jr., M. Jiang, C.-H. Lee, A. O. Stewart, H. Yu, K. L. Kohlhaas, K. M. Alexander, S. McGaraughty, J. Mikusa, K. C. Marsh, S. W. Muchmore, C. L. Jakob, E. A. Kowaluk, M. F. Jarvis and S. S. Bhagwat, *Bioorg. Med. Chem.*, 2007, **15**, 1586–1605.
- 41 A. Gomtsyan, S. Didomenico, C. H. Lee, M. A. Matulenko, K. Kim, E. A. Kowaluk, C. T. Wismer, J. Mikusa, H. X. Yu, K. Kohlhaas, M. F. Jarvis and S. S. Bhagwat, *J. Med. Chem.*, 2002, **45**, 3639–3648.
- 42 H. Weingarten, R. Martin and J. Feder, *Biochemistry*, 1985, **24**, 6730–6734.
- 43 H. Weingarten and J. Feder, *Anal. Biochem.*, 1985, **147**, 437–440.
- 44 L. J. MacPherson, E. K. Bayburt, M. P. Capparelli, B. J. Carroll, R. Goldstein, M. R. Justice, L. Zhu, S. Hu, R. A. Melton, L. Fryer, R. L. Goldberg, J. R. Doughty, S. Spirito, V. Blancuzzi, D. Wilson, E. M. O'Byrne, V. Ganu and D. T. Parker, *J. Med. Chem.*, 1997, **40**, 2525–2532.
- 45 P. Artursson and J. Karlsson, *Biochem. Biophys. Res. Commun.*, 1991, **175**, 880–885.
- 46 C. Meaney and C. O'Driscoll, *Eur. J. Pharm. Sci.*, 1999, **8**, 167–175.
- 47 *Glide, version 5.7*, Schrödinger, LLC, New York, NY, 2011.
- 48 R. A. Friesner, J. L. Banks, R. B. Murphy, T. A. Halgren, J. J. Klicic, T. Daniel, M. P. Repasky, E. H. Knoll, M. Shelley and J. K. Perry, *J. Med. Chem.*, 2004, **47**, 1739–1749.
- 49 T. A. Halgren, R. B. Murphy, R. A. Friesner, H. S. Beard, L. L. Frye, W. T. Pollard and J. L. Banks, *J. Med. Chem.*, 2004, **47**, 1750–1759.
- 50 R. A. Friesner, R. B. Murphy, M. P. Repasky, L. L. Frye, J. R. Greenwood, T. A. Halgren, P. C. Sanschagrin and D. T. Mainz, *J. Med. Chem.*, 2006, **49**, 6177–6196.
- 51 *Schrödinger Suite 2011 Protein Preparation Wizard; Epik version 2.2*, Schrödinger, LLC, New York, NY, 2011; *Impact version 5.7*, Schrödinger, LLC, New York, NY, 2011; *Prime version 3.0*, Schrödinger, LLC, New York, NY, 2011.
- 52 *LigPrep, version 2.5*, Schrödinger, LLC, New York, NY, 2011.
- 53 J. Aqvist and O. Tapia, *Biopolymers*, 1990, **30**, 205–209.
- 54 N. Díaz and D. Suárez, *Biochemistry*, 2007, **46**, 8943–8952.
- 55 C. I. Bayly, P. Cieplak, W. Cornell and P. A. Kollman, *J. Phys. Chem.*, 1993, **97**, 10269–10280.
- 56 W. D. Cornell, P. Cieplak, C. I. Bayly and P. A. Kollman, *J. Am. Chem. Soc.*, 1993, **115**, 9620–9631.

- 57 J. Wang, R. M. Wolf, J. W. Caldwell, P. A. Kollman and D. A. Case, *J. Comput. Chem.*, 2004, **25**, 1157–1174.
- 58 D. A. Case, T. A. Darden, T. E. Cheatham, III, C. L. Simmerling, J. Wang, R. E. Duke, R. Luo, R. C. Walker, W. Zhang, K. M. Merz, B. Roberts, B. Wang, S. Hayik, A. Roitberg, G. Seabra, I. Kolossváry, K. F. Wong, F. Paesani, J. Vanicek, J. Liu, X. Wu, S. R. Brozell, T. Steinbrecher, H. Gohlke, Q. Cai, X. Ye, J. Wang, M.-J. Hsieh, G. Cui, D. R. Roe, D. H. Mathews, M. G. Seetin, C. Sagui, V. Babin, T. Luchko, S. Gusarov, A. Kovalenko and P. A. Kollman, AMBER 11, 2010, University of California, San Francisco.